NRL REPORT 3534

PHYSICAL OPTICS OF METAL PLATE MEDIA
PART 1, THEORETICAL CONSIDERATIONS

Dr. B. A. Lengyel

September 19, 1949

Approved by:

Dr. L. C. Van Atta, Head, Antenna Research Branch
Dr. J. M. Miller, Superintendent, Radio Division I

NAVAL RESEARCH LABORATORY
CAPTAIN F. R. FURTH, USN, DIRECTOR
WASHINGTON, D.C.

CONTENTS

Abstract	iv
Problem Status	iv
Authorization	iv
LIST OF SYMBOLS	v
INTRODUCTION	1
Terminology and Elementary Properties	3
REFLECTION, TRANSMISSION, AND THE GRATING EFFECT	5
THE RESULTS OF CARLSON AND HEINS	6
MULTIPLE REFLECTION	10
ENERGY RELATIONS	12
MEDIA BOUNDED BY TWO PARALLEL SURFACES	13
GENERAL DISCONTINUITY RELATIONS	15
FORMULAS FOR METAL-PLATES SLABS	20
AMPLITUDE COMPUTATIONS	21
PHASE COMPUTATIONS	21
THE TABLES AND THEIR USE	26
ACKNOWLEDGMENTS	27
REFERENCES	33
APPENDIX	35

ABSTRACT

Reflection and transmission of electromagnetic plane waves at the surface of parallel-plate metal structures are studied both theoretically and experimentally. This report, Part I of the study, is the theoretical presentation; Part II will deal with apparatus and experimental findings. The study is confined to rays with polarization parallel to the edges of the plates and a plane of incidence perpendicular to these edges.

The theory of Carlson and Heins is extended and made amenable to numerical predictions. Tables and graphs are provided for the coefficients pertaining to an air-metal-plate medium interface. A method is developed for the analysis of reflecting and transmitting properties of slabs, or media of finite depth.

PROBLEM STATUS

This is an interim report; work on this problem is continuing.

AUTHORIZATION

NRL Problem No. R09-39R
NR 509-390

LIST OF SYMBOLS

Symbol	Explanation	Page first used
a	Plate separation (Fig. 1)	3
d	Thickness (depth) of slab	15
f(w)	A function defined by Eq. (7)	6
k	Phase propagation constant in free space $2\pi/\lambda$	4
$K_+(w), K_-(w)$	Functions defined by Eqs. (9) and (15)	7
n	Index of refraction	4
r	Reflection coefficient of an interface	9
R	Reflection coefficient of a slab	15
R(x)	Remainder of an infinite series, Eq. (83)	23
S	Scattering matrix Eq. (49)	17
S(y)	Remainder of an infinite series Eq. (93)	25
t	Transmission coefficient of an interface	8
T	Transmission coefficient of a slab	15
U(w)	A complex function defined by Eq. (12)	7
v	$x \sin \theta$	26
V(w)	A complex function defined by Eq. (10)	7
w	A complex variable	7
W(w)	A complex function defined by Eq. (11)	7
x	$2a/\lambda$ (Also used as a coordinate)	21
y	nx (Also used as a coordinate)	24
z	Coordinate	3
α	Angle of stacking (Fig. 1)	3
δ	Phase delay	15

LIST OF SYMBOLS (Cont.)

Symbol	Explanation	Page first used
Δ_n	Defined by Eq. (13)	7
ϵ_n	Defined by Eq. (14)	7
$\eta(s)$	$\sum_{n=4}^{\infty} (-)^n n^{-s}$	23
θ	Angle of incidence	4
θ_r, θ_2	Angle of refraction	4
θ_0	Arc cos n = arc sin $\lambda/2a$	12
θ'	Angle between the surface normal and the direction of the first order diffracted beam	11
κ	Phase propagation constant in the medium = nk	4
λ	Wavelength (in free space)	3
ρ	Magnitude of the reflection coefficient	18
ρ', ρ''	Phase of the reflection coefficient	9
τ	Magnitude of the transmission coefficient	18
τ'	Phase of the transmission coefficient	8
ψ	$\rho'' + \delta_2$	20
ω	Angular frequency	6

PHYSICAL OPTICS OF METAL-PLATE MEDIA; PART 1, THEORETICAL CONSIDERATIONS

INTRODUCTION

This report deals with certain aspects of wave propagation in the presence of the parallel-plate metal structures employed in microwave lens design. These structures consist of a set of parallel, equidistant conducting plates. They are so oriented that the polarization of the electric vector of the incident waves is parallel to the plates and the plate separation is chosen between one-half and one wavelength. When this is the case the phase velocity within the metal-plate structure is greater than in free space. This fact has been utilized by Stützer,[5,6,7] Kock,[3] and others for the construction of microwave lenses. The lenses so constructed are unusual in their appearance because the metal-plate medium has an effective index of refraction less than one, consequently convex lenses are diverging and concave ones converging.

The geometrical optics of metal-plate media has already been thoroughly explored. The present study is directed toward the exploration of the physical-optical aspects of these media.

Articles and reports dealing with microwave lens design indicate that the temptation to treat metal-plate media formally as ordinary dielectric materials has been great. While most relations of geometrical optics can be carried over formally from dielectrics to metal-plate media, this is not true of the relations of physical optics. The different behavior of the latter media is in a large part caused by the fact that energy is stored at the boundary surface of the metal-plate medium while no such storage takes place at the surface of the dielectric.

The objective of this study is to examine the reflecting and transmitting properties of metal-plate media. The ground-work in this field has already been laid by other investigators. In 1939 Stützer[5] obtained approximate expressions for the reflection and transmission coefficients for normal incidence. The wave constructions which led to these coefficients, however, do not satisfy the proper boundary conditions. Several years later Carlson and Heins[2] attacked the problem anew. They solved the field problem rigorously for any angle of incidence, requiring only that the plane of incidence be perpendicular to the metal plates. By the use of the Fourier transformation, Carlson and Heins obtained analytic expressions for the reflection and transmission coefficients which are valid when the incident radiation is subject to a number of restrictions.

An experimental program has been initiated at the Naval Research Laboratory and at Oregon State College with the purpose of testing the predictions of the theory of Carlson and Heins. The experimental program and its results are the subject of a separate report. A cursory examination of the work of Carlson and Heins is sufficient to convince one that a considerable amount of work is required to bridge the gap between the mathematical formalism

of their theory and the variables accessible to the experimenter. The theory predicts the reflection and the transmission of a plane electromagnetic wave on a single boundary surface separating free space and a metal-plate medium extending (in depth) to infinity. In the case of a medium of finite depth, the reflection from the "back" surface combines with that at the front surface. An observer can observe only the combination of these reflections unless he can eliminate all reflection at the back surface by the introduction of proper absorbing materials. In an experimental test of the theory it is then necessary either to compute reflection and transmission coefficients for media of finite depth from the single surface coefficients, or it is necessary to eliminate back surface reflections by the use of absorbing materials. Both methods have been employed, the first one primarily at the Naval Research Laboratory, the second at Oregon State College.

The first method requires the knowledge of the phase as well as the magnitude of the coefficients associated with a single surface transition. While phase relations between incident, transmitted and reflected waves are trivially simple for ordinary lossless dielectric materials, quite the opposite is true of metal-plate media. The expressions for phase relations derived by Carlson and Heins are of the form of infinite series; their numerical evaluation presented a number of difficulties. In view of this fact, the technique of the computation is described in this report and tables of the coefficients computed are appended.

Expressions for the reflection and transmission coefficients were derived by Carlson and Heins for the case when to every incident beam corresponds a single reflected beam. This condition limits the angle of incidence below a critical value determined by the ratio of wavelength to plate separation. When the critical value is exceeded, the edges of the plates act as a grating and diffracted beams arise. By extending the theory of Carlson and Heins, expressions have been found for the reflection and transmission coefficients in the presence of a diffracted beam. Tables and graphs have been prepared to show the energy distribution between various beams. The tables are not as extensive as might be desired because of limitation in time and manpower. Nevertheless those angles of incidence which are of practical value are covered.

Having obtained the basic coefficients pertaining to a single air-metal-plate medium interface it became necessary to consider the problem of composing reflections originating at the front and back surfaces of a slab, or medium of uniform depth. This is analogous to the well-known problem of reflection and transmission of transparent sheets. However, the unusual phase relations prevailing in the case of metal-plate media make certain considerations necessary which are not required in the case of ordinary dielectric materials. For this reason, a theory of the metal-plate slabs was included in this report. It is developed along the lines of the modern theory of discontinuities in transmission lines introduced by J. Schwinger.

The problems discussed in this report are less general than those of Carlson and Heins in the following respect: It is assumed here that the parallel plates are so stacked that the plane containing their edges is perpendicular to the plates, while Carlson and Heins permit this plane to make any angle with the plates. Perhaps the most serious limitation of this work is that it had been confined to a plane of incidence perpendicular to the edges of the plates. This is the plane of the maximum constraint from the point of view of wave propagation within the medium. The examination of other planes of incidence and other orientations of polarization is in progress.

Terminology and Elementary Properties

A parallel-plate or metal-plate medium is a part of space containing a number of parallel, equidistant, highly conducting sheets. Such a structure is shown in Figure 1 with the plates perpendicular to the plane of the paper.

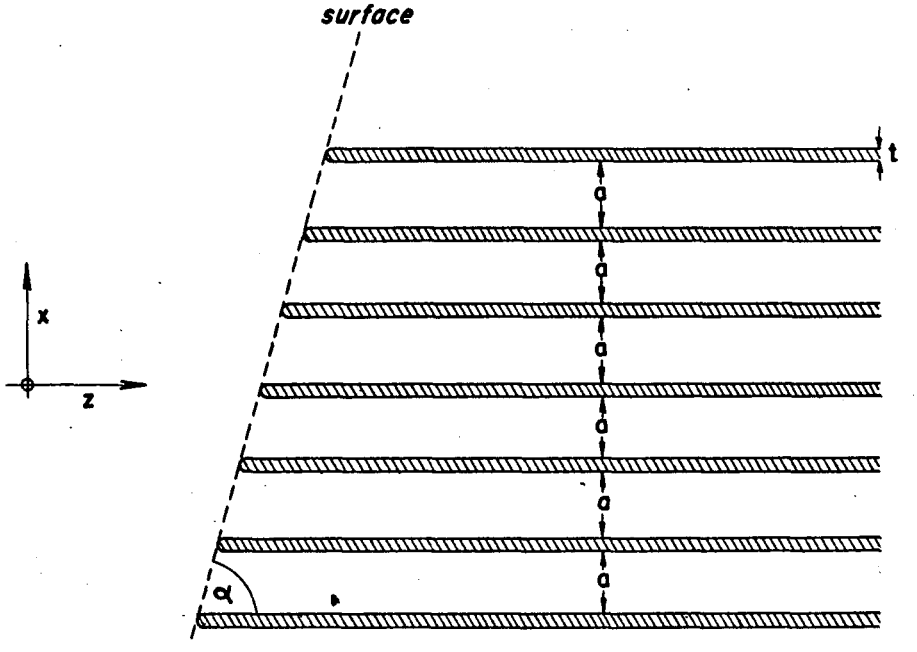

Fig. 1 - Parallel plate medium (side view)

It is assumed that the plates extend to infinity forward, back, and to the right, that the edges of the plates are straight and perpendicular to the paper, that the plates are stacked uniformly as shown in Figure 1. Moreover, to avoid the complications caused by edge effects, it is assumed that there are many plates and that the investigation is confined to the center part of the structure so that one plate is not distinguished physically from the adjacent ones by virtue of its position. In mathematical parlance this assumption is expressed by postulating an infinite number of plates, located at the points satisfying the conditions $z \leq x \cot\alpha$, $x = ma$, $m = 0, \pm 1, \pm 2, \ldots$. The plane through the edges of the planes is called the surface of the medium.

The parameters determining the electrical properties of the medium are the plate separation a, the plate thickness t, the conductivity σ and the shape of the surface of the medium determined by the angle of stacking α. The propagation of electromagnetic waves within the medium is determined by a and σ; the effect of the latter being usually negligible. Surface phenomena, such as reflection of an incident wave will depend on α and t also.

Metal-plate media are generally intended for use in a well-defined frequency region and the parameters of the structure are so chosen that t is very small compared to the wavelength λ, a is of the same order as λ and σ is that of ordinary metals (5×10^7 mhos meter). In first approximation one always assumes $t = 0$ and $\sigma = \infty$. To avoid complications, this study is restricted to the case $\alpha = 90^\circ$.

Only those electromagnetic waves will be considered whose electric vector is parallel to the metal plates. The plate separation is generally so chosen that at the given frequency only one mode of oscillation is propagating in the medium. This condition requires

$$1 \leqq \frac{2a}{\lambda} < 2. \tag{1}$$

It is well-known that there is no propagation within the medium for $\lambda > 2a$ and that for $\lambda < 2a$ the ratio of the phase velocity in free space to the phase velocity in the medium is

$$n = \sqrt{1 - \left(\frac{\lambda}{2a}\right)^2}\,. \tag{2}$$

This quantity is called the <u>index of refraction</u> of the medium. Let k be the propagation constant in free space; $k = 2\pi/\lambda$, and let $\kappa = nk$ be the corresponding quantity in the medium. Equation (2) is equivalent to

$$k^2 = \kappa^2 + \left(\frac{\pi}{a}\right)^2. \tag{3}$$

The value of n determines the propagation within the plates and also the geometrical optics of the rays incident on the surface of the medium. Rays incident in a plane parallel to that of the plates are not constrained, while rays incident in other planes are all constrained by the plates. The classical argument pertaining to the propagation of phase fronts shows that unconstrained rays follow Snell's law. When rays are incident in the plane of maximum constraint, the (x,z) plane, the Poynting vector in the medium is always directed along the z-axis. Still one might speak of refraction at the surface in terms of equiphase surfaces. Consider the case when the plates are not staggered; i.e., $\alpha = 90^0$, and let the radiation be incident at an angle θ as shown in Figure 2. The points P_0, P_1, P_{-1}, etc. will lie on a discontinuous equiphase surface which is approximated by the plane shown in dotted lines. Let the inclination of this plane be θ_r. Elementary calculation gives

$$\frac{\sin\theta}{\tan\theta_r} = n. \tag{4}$$

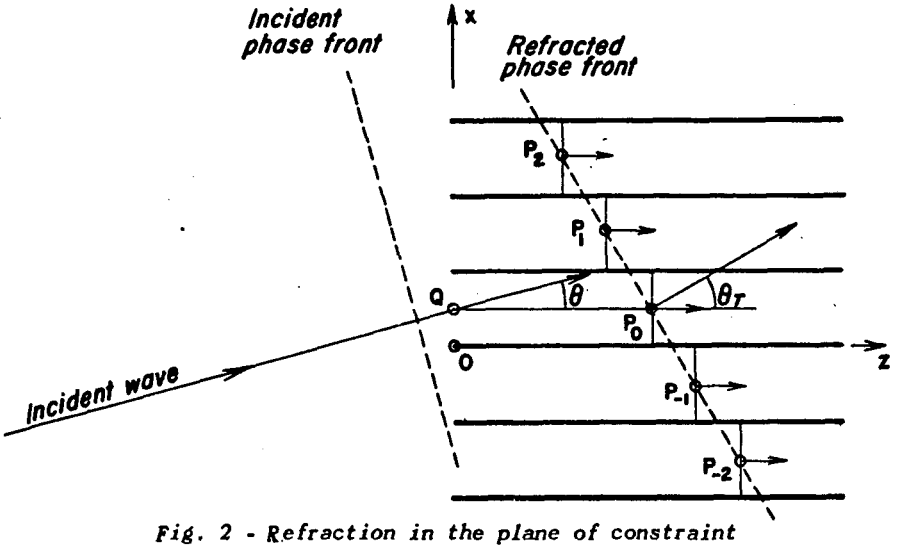

Fig. 2 - Refraction in the plane of constraint

REFLECTION, TRANSMISSION, AND THE GRATING EFFECT

When a plane wave is incident on the surface of a metal-plate medium, currents are induced on the plates. In addition to waves set up in the medium there will be reflected or scattered waves in free space. Analogy with dielectric materials leads one to expect a transmitted and a reflected plane wave. However, the analogy is an incomplete one since the situation at the surface of the metal-plate medium differs in many respects from that encountered at the surface of dielectrics.

First of all, the electric field at the surface of a metal-plate medium is not uniform, but a periodic function of position. Therefore, transmitted and reflected waves cannot be uniform plane waves as they are in the case of dielectrics. Only at a distance from the surface might one expect approximately uniform plane waves.

There is never more than one reflected wave from a plane dielectric surface, but the edges of the metal-plates act as a grating and for a single plane wave incident at an angle θ, there will be reinforcement of scattered waves in all directions θ_S which satisfy the relation

$$\sin\theta + \sin\theta_S = m\frac{\lambda}{a}, \quad m = 0, \pm 1, \pm 2, \ldots \quad . \tag{5}$$

There will always be the beam $\theta_S = -\theta$ corresponding to $m = 0$. This is the case of common (specular) reflection in geometrical optics. There might be other beams, provided that the elements of the grating are sufficiently far apart. However, when

$$1 + |\sin\theta| < \frac{\lambda}{a} \tag{6}$$

then (5) cannot be satisfied for any value of m other than zero; thus there is only one reflected beam. Since $\alpha = 90^0$ has already been assumed, one may, without further loss of generality, restrict himself to positive angles of incidence and omit the absolute value signs in (6).

The electromagnetic disturbance caused by the incident plane wave at the surface of the medium results in oscillations in the space between the plates. The latter act as waveguides of uniform width and infinite height. They permit the passage of an oscillation of a given frequency in several modes propagating with different velocities. In all applications the spacing a is chosen to satisfy the inequality (1), so that in the contemplated frequency range only the fundamental mode is propagated. All other modes excited at the edges are attenuated. The energy associated with these nonpropagating modes is stored in the part of the space surrounding the edges. The presence of this energy is responsible for the phase shift in transmission through the surface of the metal-plate medium. If one overlooks the field present in these higher modes he is led to erroneous boundary conditions in the process of joining the incident, reflected and propagated waves by means of a continuity argument. These conditions in turn lead to incorrect reflection and transmission coefficients.[5]

A rigorous theory of metal-plate media is quite difficult and has not yet been fully developed. Carlson and Heins[2] solved the problem for the case of a plane wave incident in the plane of maximum constraint assuming infinite conductivity and zero plate-thickness. Their mathematical procedure is far too complicated for reproduction here. Only the principal results will be stated for the special case $\alpha = 90^0$.

THE RESULTS OF CARLSON AND HEINS†

After formulating the electromagnetic field problem in terms of an integral equation of the Wiener-Hopf type, Carlson and Heins proceed to solve this equation by the use of the Fourier transform. The crucial step in the solution requires the splitting of a complex transcendental function in two parts; one of which has no zeros or poles in the upper half-plane, the other is similarly behaved in the lower half-plane. The function in question is (for $\alpha = 90^0$)

$$f(w) = \frac{\sin a\sqrt{k^2 - w^2}}{\sqrt{k^2 - w^2}\left[\cos a\sqrt{k^2 - w^2} - \cos(ak \sin\theta)\right]} \tag{7}$$

It is written in the form

$$f(w) = \frac{K_-(w)}{K_+(w)}, \tag{8}$$

where $K_-(w)$ has no poles or zeros below the line C in Figure 3 and $K_+(w)$ has none above.

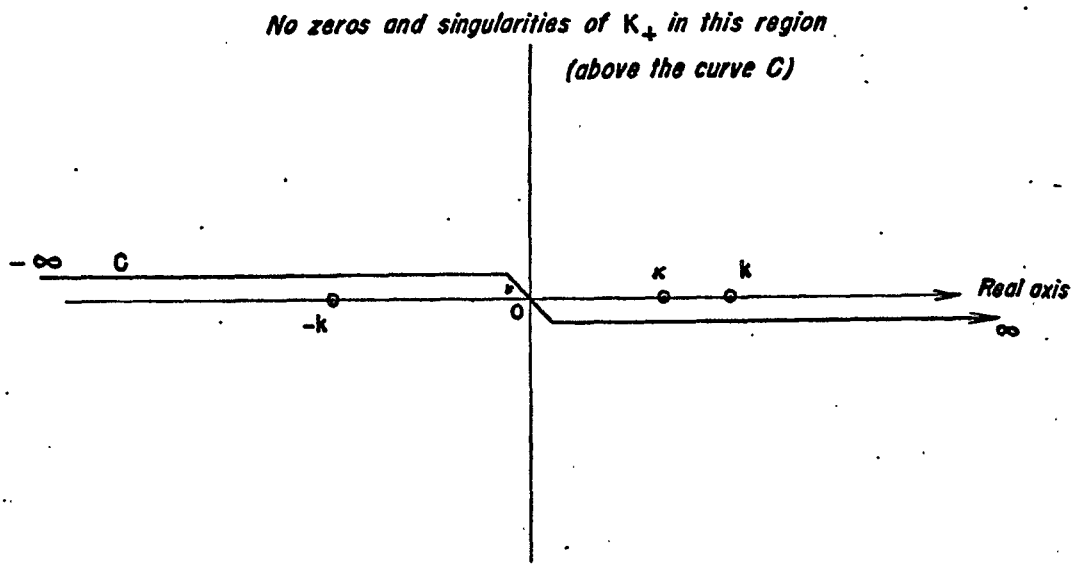

Fig. 3 - The plane w

†*For a complete understanding of the next two sections, it is helpful to read the article of Carlson and Heins.*[2] *In order to facilitate a comparative reading, the convention of using a time dependence in the form of* $e^{-i\omega t}$ *has been retained in this section. Consequently, the reflection coefficient is written in the form of* $r = |r|\, e^{i\rho}$. *To convert to the standard notation used in other parts of this report it is only necessary to replace i by −j.*

The functions are properly normalized to insure desired behavior at infinity. The actual form of $K_+(w)$ is

$$K_+(w) = \frac{\pi}{2} \frac{w + k\cos\theta}{w + \kappa} \frac{V(w)\,W(w)}{U(w)} \exp\left\{\frac{iaw}{\pi}(\ln 2 - 1)\right\}, \tag{9}$$

where

$$V(w) = \prod_{n=1}^{\infty} \left(\Delta_n - \frac{iaw}{2\pi n}\right) \exp\left\{\frac{iaw}{2\pi n} + \frac{ak\sin\theta}{2\pi n}\right\}, \tag{10}$$

$$W(w) = \prod_{n=-1}^{-\infty} \left(\Delta_n + \frac{iaw}{2\pi n}\right) \exp\left\{-\frac{iaw}{2\pi n} + \frac{ak\sin\theta}{2\pi n}\right\}, \tag{11}$$

$$U(w) = \prod_{n=2}^{\infty} \left(\epsilon_n - \frac{iaw}{\pi n}\right) \exp\left\{\frac{iaw}{\pi n}\right\}, \tag{12}$$

with

$$\Delta_n^2 = \left(1 - \frac{ak\sin\theta}{2\pi n}\right)^2 - \left(\frac{ak}{2\pi n}\right)^2, \tag{13}$$

$$\epsilon_n^2 = 1 - \left(\frac{ak}{\pi n}\right)^2. \tag{14}$$

In order to insure proper behavior of U, V and W in the upper half-plane, the sign of Δ_n and ϵ_n has to be determined as follows: When $\Delta_n^2 \geq 0$, then $\Delta_n \geq 0$, when $\Delta_n^2 < 0$, then $i\Delta_n > 0$. On account of the restriction expressed by (1), ϵ_n^2 is always positive and the correct choice is $\epsilon_n > 0$. The numerator of (8) then takes the form:

$$K_-(w) = \frac{a}{\pi} \frac{w - \kappa}{w - k\cos\theta} \frac{U(-w)}{V(-w)W(-w)} \exp\left\{\frac{iaw}{\pi}(\ln 2 - 1)\right\}. \tag{15}$$

Assuming an incident field of the form $E_x = 0$, $E_z = 0$, $E_y = \phi_{inc} = \exp\{ik(x\sin\theta + z\cos\theta)\}$ the total electric field is represented by the following equation:

$$\phi(x, z) = \phi_{inc} + \frac{1}{2\pi i}\int_C \frac{K_+(k\cos\theta)\, I(w, x)\, e^{iwz}\, dw}{K_+(w)(w - k\cos\theta)\sin a\sqrt{k^2 - w^2}}, \tag{16}$$

where

$$I(w, x) = \left[\sin(x - n'a - a)\sqrt{k^2 - w^2} - e^{ika\sin\theta} \sin(x - n'a)\sqrt{k^2 - w^2}\right] e^{in'ka\sin\theta} \tag{17}$$

and n′ is the largest integer not exceeding x/a. This is the special case ($\alpha = 90°$) of the principal result of Carlson and Heins (p. 325). The path of integration is shown in Figure 1.†

The reflected and transmitted fields are obtained from (16) evaluated for negative and positive values of z respectively. One can show that the behavior of the integrand in (16) is such that the curve C can be closed by a large semicircle in the upper half-plane for positive values of z and by a similar semicircle in the lower half-plane for negative values of z. The contributions from these circular arcs vanish as their radii tend to infinity. It is therefore possible to evaluate the integral in (16) by means of the theorem of residues, the poles of the integrand being $w_0 = k \cos\theta$, the zeros of $K_+(w)$ and those zeros of $\sin a\sqrt{k^2 - w^2}$ which are not cancelled by the numerator of the integrand.

In the case of the transmitted wave, z is positive, the path of integration is closed in the upper half-plane, therefore only poles situated above C need to be considered. Since $K_+(w)$ has no zeros in this region, the poles are at $w_0 = k\cos\theta$ and at such points w_m in the upper half-plane which satisfy the equation $a\sqrt{k^2 - w_m^2} = m\pi$, where m is a positive integer. The restriction of single mode propagation within the medium, expressed by the inequality (1), has the consequence that all w_m with $m > 1$ are pure imaginary, while $w_1 = (k^2 - \pi^2/a^2)^{1/2} = \kappa$. For $m > 1$ it is then proper to write $w_m = ip_m$, where $p_m > 0$. The expression obtained by evaluating the residue at w_m will contain the factor $e^{-p_m z}$, indicating a nonpropagating wave. Only real poles generate propagating waves. In fact, the residue at w_0 generates $-\phi_{inc}$, the one at $w = \kappa$ generates $t\,e^{i\kappa z}\sin(\pi x/a)$, where

$$t = (-)^{n'+1}\,\frac{\pi}{a^2\kappa}\,\frac{K_+(w_0)}{K_+(\kappa)}\,\frac{1 + e^{ika\sin\theta}}{(\kappa - w_0)}\,e^{in'ak\sin\theta}\,. \tag{18}$$

The factor $e^{in'ak\sin\theta}$ takes into account the phase delay from one channel of the medium to the next. It is sufficient to concentrate on a particular pair of plates and to examine only the field between them. In this case one may set $n' = 0$ and simplify the expression of the transmission coefficient to:

$$t = |t|\,e^{i\tau'} = \frac{\pi}{a^2\kappa}\,\frac{K_+(k\cos\theta)}{K_+(\kappa)}\,\frac{1 + e^{ika\sin\theta}}{k\cos\theta - \kappa}\,. \tag{19}$$

Assuming that all deltas defined by (13) are real, one obtains after a lengthy calculation:‡

$$|t| = \frac{2^{3/2}\,k\cos\theta}{k\cos\theta + \kappa} = \frac{2^{3/2}\cos\theta}{\cos\theta + n}\,, \tag{20}$$

where n is the index of refraction defined in (2).

For the phase of the transmission coefficient (19) yields readily:

$$\tau' = \frac{1}{2}\,a\,k\sin\theta + \arg K_+(k\cos\theta) - \arg K_+(\kappa), \tag{21}$$

---

† *Actually Carlson and Heins used a k with a positive imaginary part, integrated along the real axis and then permitted Im k to approach zero. The location of their path of integration with respect to the singularities is identical to that shown in Figure 3.*

‡ *See Appendix, Eqs. (4A) and (6A).*

provided $\cos\theta > n$ which is usually the case. The first term in this expression is due to the location of the origin. It disappears when the origin is shifted to a point half-way between the edges, such as Q in Figure 2.

The reflection coefficient is obtained by evaluating the integral in (16) for large negative values of z. In this case the path of integration is closed in the lower half-plane.

If the quantities Δ_n, defined by (13) are all real, then, apart from $w = -k\cos\theta$, $K_+(w)$ has only pure imaginary roots in the lower half-plane. The latter generate attenuated waves as was shown before. The roots of $\sin a\sqrt{k^2 - w^2}$ in the lower half-plane are cancelled by the poles of $K_+(w)$, therefore there is one propagating reflected wave. It is of the form:

$$r\, e^{ik(x\sin\theta - z\cos\theta)} \tag{22}$$

with

$$r = |r|\, e^{i\rho'} = -\frac{K_+(k\cos\theta)}{2k\cos\theta\, K_+'(-k\cos\theta)}, \tag{23}$$

where K_+' is dK_+/dw. Equation (23) gives:

$$\rho' = \arg K_+(k\cos\theta) - \arg K_+'(-k\cos\theta) + \pi. \tag{24}$$

When the deltas in the functions V and W are all real, $|r|$ can be computed by elementary means. In this case:†

$$\left|\frac{K_+(k\cos\theta)}{K_+'(-k\cos\theta)}\right| = 2k\cos\theta\left|\frac{-k\cos\theta + \kappa}{k\cos\theta + \kappa}\right|, \tag{25}$$

and hence from $\kappa = nk$ and equation (23) follows

$$|r| = \frac{\cos\theta - n}{\cos\theta + n}. \tag{26}$$

The absolute value sign has been omitted on the right because the restriction on the deltas implies $\cos\theta > n$. This will be shown immediately. First, it is proper to examine the meaning of the restrictions $\Delta_n^2 \geqq 0$ for all values of n. For negative values of n, Δ_n^2 is positive for every angle of incidence θ (in the first quadrant). This is a consequence of condition (1), imposed to insure single mode propagation between the plates. The condition $\Delta_n^2 \geqq 0$ for positive n is, however, more restrictive. Since $\Delta_n^2 < \Delta_{n+1}^2$, only Δ_1^2 needs to be examined. The latter is not negative if, and only if,

$$1 - \frac{ka}{2\pi}\sin\theta \geqq \frac{ka}{2\pi}, \tag{27}$$

or

$$\frac{\lambda}{a} = \frac{2\pi}{ka} \geqq 1 + \sin\theta. \tag{28}$$

---

†*The factors resulting from the infinite products cancel out, since for any real number w_o, $|V(-w_o)| = |V(w_o)|$, $|W(-w_o)| = |W(w_o)|$ when all deltas are real and $|U(-w_o)| = |U(w_o)|$ because the epsilons are always real on account of condition (1). The evaluation of K_+ in the general case is discussed in the Appendix.*

This is the inequality (6) derived from the elementary grating theory. It restricts the angle of incidence θ to such values which permit only a single reflected beam. Equations (20) and (26) are valid only when θ satisfies this condition. The limiting value of θ for which the equality sign holds is shown in Figure 4 as a function of $2a/\lambda$.

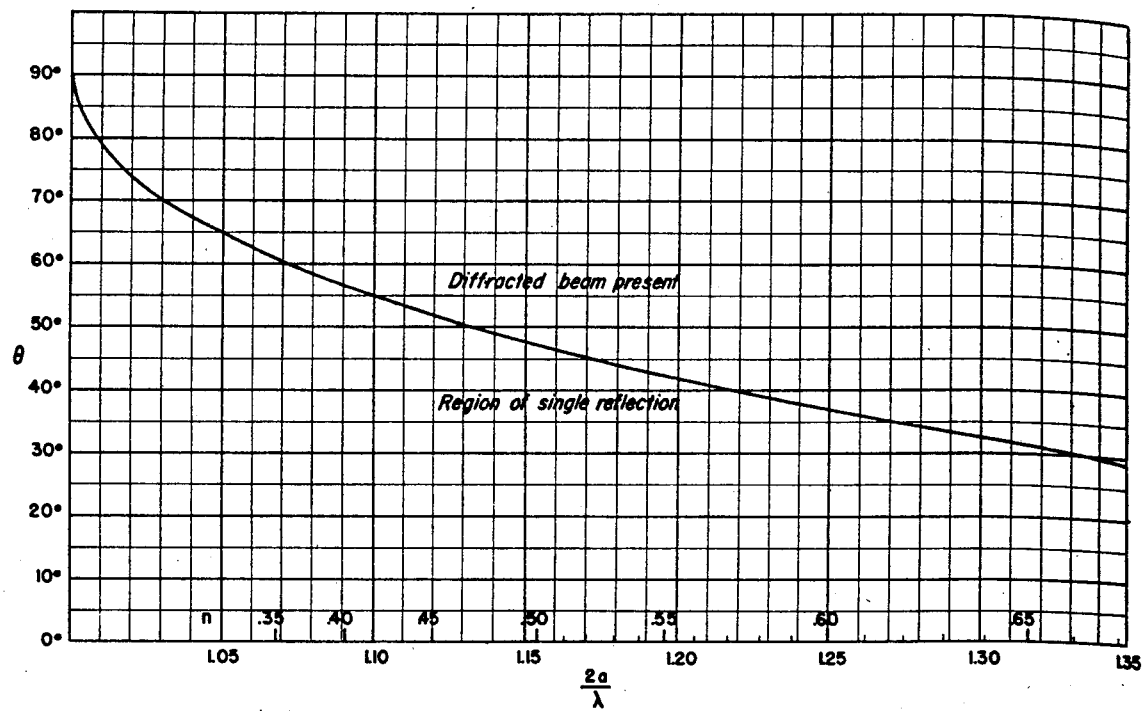

Fig. 4 - Limiting valve of angle of incidence for single reflection

$$\theta_L = \arcsin\left(\frac{\lambda}{a} - 1\right)$$

The inequality $\cos\theta > n$ now follows readily. From (28):

$$1 - \sin\theta > 2 - \frac{\lambda}{a} = 2\left(1 - \frac{\lambda}{2a}\right). \tag{29}$$

For any positive θ

$$1 + \sin\theta > 1 = 2.\tfrac{1}{2} \tag{30}$$

and according to (1), $2 > 1 + \lambda/2a$, therefore

$$1 + \sin\theta > \tfrac{1}{2}(1 + \lambda/2a). \tag{31}$$

The desired relation is the product of the inequalities (29) and (31).

MULTIPLE REFLECTION

It is worth while to extend the theory of Carlson and Heins to cover the case of multiple reflected beams. The case of most importance is the one of two reflected beams. This

corresponds to an angle of incidence θ for which $\Delta_1^2 < 0$, but $\Delta_2^2 > 0$. According to (13)

$$-\Delta_1^2 = \left(\frac{ak}{2\pi}\right)^2 \left\{1 - \left(\frac{2\pi}{ak} - \sin\theta\right)^2\right\}. \tag{32}$$

Clearly $-\Delta_1^2 < (ak/2\pi)^2$, therefore whenever $\Delta_1^2 < 0$ there is an angle θ' such that

$$\Delta_1 = -i\,\frac{ak}{2\pi}\cos\theta'. \tag{33}$$

From (32) then follows

$$\pm\sin\theta' = \frac{2\pi}{ak} - \sin\theta. \tag{34}$$

It is proper to restrict oneself to the use of the + sign in (34) since (33) does not specify the sign of θ'. Then

$$\sin\theta + \sin\theta' = \frac{2\pi}{ak} = \frac{\lambda}{a}. \tag{35}$$

The function $K_+(w)$ now has an additional real root, since the factor $\Delta_1 - iaw/2\pi$ vanishes when $w = -k\cos\theta'$. When the presence of this real pole is taken into account in the evaluation of the integral in (16), a new propagating wave is found in the region $z < 0$. In fact, from (17) and (35) follows $I(-k\cos\theta', x) = -\sin(ak\sin\theta')\exp(-ikx\sin\theta')$ and the contribution of the pole is $r^{(1)}\exp\{-ik(x\sin\theta' + z\cos\theta')\}$, where

$$r^{(1)} = -\frac{K_+(k\cos\theta)}{K_+'(-k\cos\theta')}\,\frac{1}{k(\cos\theta + \cos\theta')}. \tag{36}$$

This is the first order diffracted beam; it propagates at an angle θ' with the surface normal.

The quantities necessary for the calculation of $|t|$, $|r|$ and $|r^{(1)}|$ are evaluated in the Appendix for the case when $\Delta_1^2 \leqq 0$, but $\Delta_2^2 > 0$. The following expressions result:

$$|t| = \frac{2^{2/3}\cos\theta}{\cos\theta + n}\sqrt{\frac{\cos\theta' - n}{\cos\theta' + n}\,\frac{\cos\theta' + \cos\theta}{\cos\theta' - \cos\theta}}, \tag{37}$$

$$|r| = \frac{\cos\theta - n}{\cos\theta + n}\,\frac{\cos\theta + \cos\theta'}{\cos\theta - \cos\theta'}, \tag{38}$$

$$|r^{(1)}| = \frac{2\cos\theta}{|\cos\theta' - \cos\theta|}\sqrt{\frac{\cos\theta - n}{\cos\theta + n}\,\frac{n - \cos\theta'}{n + \cos\theta'}}. \tag{39}$$

These equations are valid for those angles of incidence θ which satisfy the inequalities:

$$\frac{\lambda}{a} < 1 + \sin\theta < \frac{2\lambda}{a}. \tag{40}$$

They can be put in a symmetrical form by the introduction of the angle $\theta_0 = \arccos \mathbf{n}$.

It is interesting to examine these coefficients for the angle of incidence $\theta = \theta_0$. From $\cos\theta_0 = \mathbf{n}$ follows $\sin\theta_0 = \lambda/2a$. Then (35) takes the form:

$$\sin\theta + \sin\theta' = 2\sin\theta_0. \tag{41}$$

Therefore, if two of the angles θ, θ', θ_0 are equal, then all the three are equal. The expressions (37), (38), and (39) are of the indeterminate form 0/0 for $\theta = \theta_0$.

On evaluating $\lim\limits_{\theta\to\theta_0} \dfrac{\cos\theta - \cos\theta_0}{\cos\theta' - \cos\theta}$ according to L'Hospital's rule and noting that

$d\theta'/d\theta = -1$ when $\theta = \theta'$, one obtains $|r| = 1/2$ for $\theta = \theta_0$. By comparing (23) and (36) it is clear that $|r|$ and $|r^{(1)}|$ must be equal for $\theta = \theta'$, therefore $|r^{(1)}| = 1/2$. A brief calculation yields $|t| = 1$.

ENERGY RELATIONS

Since the experiments are generally so designed that energy flow and not amplitude is detected, it is of practical value to derive expressions for the former. The quantity $p_r = |r|^2$ is a correct measure of the relative power in the beam reflected according to the law of geometrical optics. The quantity $|t|$ is the maximum of the electric vector between a pair of plates, the space variation being sinusoidal. Thus the average rate of energy flow in the direction of the z-axis is $\frac{1}{2}\mathbf{n}|t|^2$. The change in cross section of the beam at the surface introduces a factor $\sec\theta$, therefore the relative transmitted power is:

$$p_t = \frac{1}{2}\mathbf{n}|t|^2 \sec\theta = \frac{4\,\mathbf{n}\cos\theta}{(\mathbf{n}+\cos\theta)^2} \tag{42}$$

for the range specified by (28) and

$$p_t = \frac{4\,\mathbf{n}\cos\theta}{(\mathbf{n}+\cos\theta)^2}\,\frac{\cos\theta' - \mathbf{n}}{\cos\theta' + \mathbf{n}}\,\frac{\cos\theta' + \cos\theta}{\cos\theta' - \cos\theta} \tag{43}$$

for the range specified by (40).

In general, there is a change in cross section in the case of the diffracted beam. Therefore

$$p_r^{(1)} = \frac{\cos\theta'}{\cos\theta}\left|r^{(1)}\right|^2, \tag{44}$$

when θ satisfies (40) and $p_r^{(1)} = 0$ when θ satisfies (28).

The quantities p_r, $p_r^{(1)}$ and p_t describe the division of power incident on a surface element of an air-metal-plate medium interface of infinite extent. The conservation of energy requires $p_r + p_r^{(1)} + p_t = 1$. Figure 5 shows the variation of power division with angle of incidence for $2a/\lambda = 1.10, 1.20, 1.30$ and 1.40.

When $\theta = \theta' = \theta_0$, the $p_r = p_r^{(1)} = 1/4$ and $p_t = 1/2$; i.e., one-half of the energy is transmitted into the metal-plate medium, the other half is equally divided between two beams located symmetrically about the surface normal.

L. J. Chu† previously deduced this division of power for $\theta = \theta_0$ by elementary considerations. He wrote the incident wave in the form

$$\begin{aligned}\phi_{inc} &= \exp\left\{ik(z\cos\theta_0 + x\sin\theta_0)\right\} = \exp\left\{iknz\right\}\exp\left\{i\pi x/a\right\} \\ &= \exp\left\{inkz\right\}\cos\pi x/a + i\exp\left\{iknz\right\}\sin\pi x/a.\end{aligned} \tag{45}$$

Each term on the right of (45) corresponds to a wave carrying one-half of the energy. The second term satisfies the boundary conditions within the metal-plate medium; it is the transmitted wave. The first term represents a wave antisymmetric about the plane $x = a/2$; it is responsible for the storage of energy at the interface and for the presence of reflected waves. By elementary symmetry considerations one can deduce that the reflected waves make equal angles with the surface normal and carry equal amounts of power.

It is of some interest to note that if the index of refraction of a metal-plate structure is chosen large for the purpose of reducing reflection at normal incidence, the advantage so gained is quickly lost when the same structure is illuminated at an angle which permits the appearance of a diffracted beam. This is born out by Figure 5.

MEDIA BOUNDED BY TWO PARALLEL SURFACES

The theory described in the preceding section gives the reflection and the transmission coefficients of the air-metal-plate interface. In any experimental test in which the energy propagating between the plates is not completely absorbed, it is necessary to take into account the multiple reflections within the parallel-plate structure. A metal-plate medium of finite uniform depth bounded by plane surfaces will be called a metal-plate slab. The reflection from such a slab depends on the reflection coefficients of the front and of the back surfaces and on the distance between these surfaces.

From the point of view of theory, the basic quantities are the coefficients describing the air-metal-plate interface. The experimenter, however, always operates with slabs or other shapes of finite depth. It is possible to reduce greatly the effect of multiple reflections by constructing deep slabs containing absorbing wedges, but some uncertainty with regard to the phase and magnitude of the back surface reflections still remains. It is therefore desirable to deduce expressions describing the behavior of slabs, or metal-plate media bounded by two parallel surfaces.

The corresponding problem has been solved in connection with dielectric sheets and lossless transmission lines. Let r_1 be the reflection coefficient and t_1 the transmission

† *Oral communication; see Acknowledgments.*

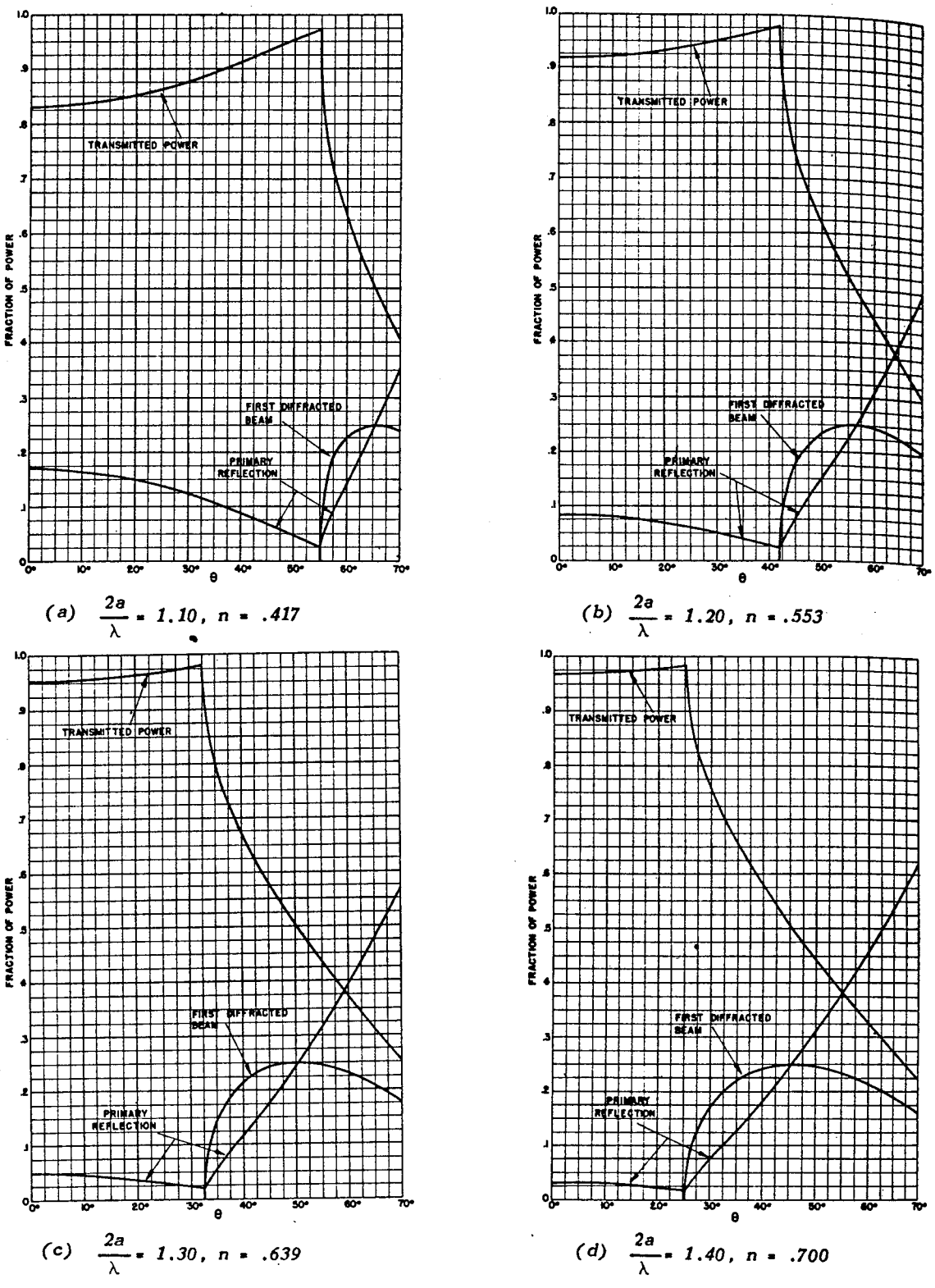

(a) $\frac{2a}{\lambda} = 1.10,\ n = .417$

(b) $\frac{2a}{\lambda} = 1.20,\ n = .553$

(c) $\frac{2a}{\lambda} = 1.30,\ n = .639$

(d) $\frac{2a}{\lambda} = 1.40,\ n = .700$

Fig. 5 - Power distribution as a function of angle of incidence

coefficient of the interface separating media 1 and 2 when the radiation is incident from medium 1 (usually air) and let r_2 and t_2 have similar meanings for a radiation incident from medium 2. These quantities will in general depend on the angle of incidence θ. To distinguish coefficients pertaining to the slab from those pertaining to single surfaces, the former will be denoted by capital letters. One can show that the reflection coefficient of a slab of medium 2 surrounded on both sides by medium 1 is given by the equation†

$$R = r_1 + \frac{r_2 t_1 t_2 \exp\left\{-2j\delta_2\right\}}{1 - r_2^2 \exp\left\{-2j\delta_2\right\}}, \tag{46}$$

where δ_2 is the phase delay between the two intersections of a normal of the slab with the surfaces. In the case of a lossless dielectric slab of thickness d and of refractive index n one has $\delta_2 = dk_2 \cos\theta_2$, where $k_2 = nk_1 = 2\pi n/\lambda$ and θ_2 is the angle of refraction.

Similarly, for the transmission coefficient one finds in the literature

$$T_1 = \frac{t_1 t_2 \exp\left\{-j\delta_2\right\}}{1 - r_2^2 \exp\left\{-2j\delta_2\right\}}. \tag{47}$$

A few words of caution about the phases of these coefficients are in order. The coefficient R refers to the front surface of the slab. If the plane of reference is chosen elsewhere, say in the plane of symmetry of the slab, the phase of R must be altered. Equation (47) gives the phase of the transmitted wave at (x, y, d + 0) with respect to the phase of the incident wave at (x, y, 0), and not the change of phase produced by the introduction of the slab into the path of the radiation. If the latter is desired, one has to multiply T_1 by $\exp j\delta_1$, where δ_1 is the phase delay through a slab of thickness d made of medium 1. When medium 1 is air, which is usually the case, $\delta_1 = 2\pi d \cos\theta/\lambda$.

Let the incident wave be of the form $\exp\left\{-jk(z\cos\theta + \sin\theta)\right\}$ ‡and let the slab be bounded by the planes z = 0 and z = d. The reflected wave will then have the form $R \exp\left\{-jk(-z\cos\theta + x\sin\theta)\right\}$ and the transmitted wave in the region z > d will have the form $T \exp\left\{-jk(z\cos\theta + x\sin\theta)\right\}$, where $T = T_1 e^{j\delta_1}$. For slabs bounded on both sides by the same medium, the coefficient T seems more fundamental than T_1, although the latter is more commonly found in the literature. T does not depend on a plane of reference; it compares the wave in the presence of the slab with the wave in its absence.

The principal difference between dielectric slabs and metal-plate slabs is that in the case of the latter the single surface coefficients r_1, r_2, t_1 and t_2 are not real. The simple equations connecting these quantities must be replaced by new ones. These will now be derived for the case when the angle of incidence is such that there is only one reflected beam. The discussion can be made general so as to include lossless dielectric slabs, and discontinuities in transmission lines as well.

GENERAL DISCONTINUITY RELATIONS

Let the plane z = 0 be a locus of discontinuity for the propagation of electromagnetic waves. This plane might be the boundary of two dielectric media, the surface of a

†*Ref. 1, p. 355.*

‡*The time dependence is exp jωt.*

metal-plate medium, a place where the dimensions of a transmission line undergo a sudden change, etc. In general, the propagation constants on the two sides of the discontinuity will be different.

To simplify matters it is practical at this point to exclude multiple propagation and multiple reflection. While in the neighborhood of the discontinuity energy might be stored in the form of "higher" modes, it is assumed that far away from the discontinuity on either side there is only one wave propagating toward and one away from the discontinuity. The case of plane waves arriving at the plane $z = 0$ at oblique angles of incidence is included in this discussion. To each angle of incidence θ_1 in the medium to the left of the discontinuity the law of refraction orders an angle θ_2 in the medium to the right. The four waves to be considered together have the directions of propagation θ_1, $\pi - \theta_1$, θ_2, $\pi - \theta_2$. These are shown in Figure 6.

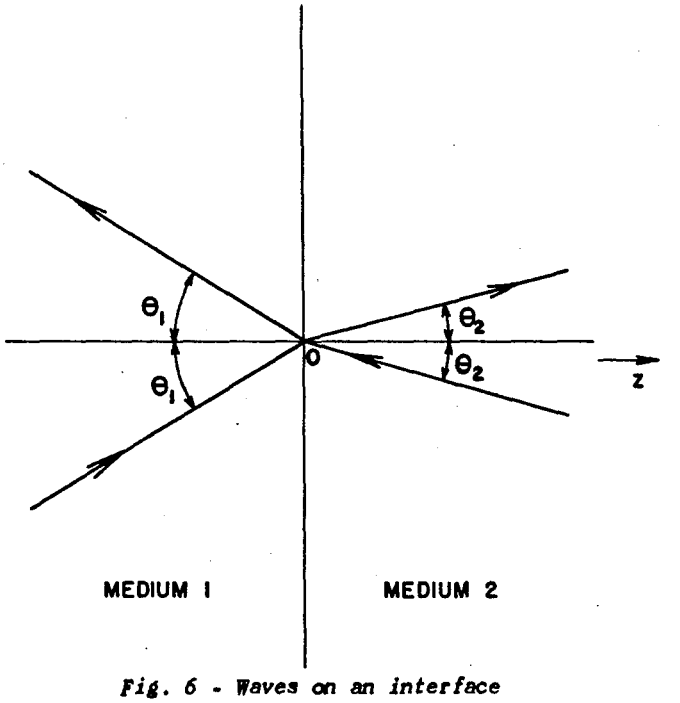

Fig. 6 - Waves on an interface

It is appropriate then to observe the discontinuity from far away on both sides, so far that one has to deal with a pair of waves on each side. Formally such a system is identical with a two-terminal pair network. The plane (or propagating) waves observed far from the discontinuity can then be extended mathematically to the plane $z = 0$, and one might speak of the amplitude of the plane wave at $z = 0$ even though a very complex field exists in the latter neighborhood. When for large negative values of z one has a wave of the asymptotic form $b_1 \exp\{jkz\}$, the quantity b_1 will be regarded as the amplitude of this wave at $z = 0$. This is the customary procedure employed in discussion of discontinuities in waveguides.[4]

Let a_1 and a_2 be complex numbers proportional to the electric amplitudes at $z = 0$ of the waves traveling toward the discontinuity and let b_1 and b_2 have a similar meaning for waves traveling away from the discontinuity. The subscripts are indicative of the media 1 (left) and 2 (right). Let **a** be a vector with components a_1 and a_2 and let **b** have a similar meaning.

On account of the linear character of Maxwell's equations and the boundary conditions the vector **b** depends on **a** linearly:

$$\mathbf{b} = \mathbf{S}\mathbf{a}. \tag{48}$$

The scattering matrix **S** connects the incoming and the outgoing waves. It is easy to see that

$$\mathbf{S} = \begin{pmatrix} r_1 & t_2 \\ t_1 & r_2 \end{pmatrix} \tag{49}$$

It has been shown that when the vectors a and b are properly normalized, the matrix **S** is symmetrical.†

When no dissipation of energy takes place at the discontinuity the conjugate matrix **S*** is the inverse of **S**.‡ In symbols:

$$\mathbf{S}\mathbf{S}^* = \mathbf{I}, \tag{50}$$

where I is the identity matrix.§

The matrix equation (50) is equivalent to the following four scalar equations:

$$|r_1|^2 + t_2 t_1^* = 1, \tag{51}$$

$$|r_2|^2 + t_1 t_2^* = 1, \tag{52}$$

$$r_1 t_2^* + t_2 r_2^* = 0, \tag{53}$$

$$t_1 r_1^* + r_2 t_1^* = 0. \tag{54}$$

From (51) and (52) follows:

$$|r_1|^2 - |r_2|^2 = t_1 t_2^* - t_1^* t_2 = 2 \operatorname{Im} t_1 t_2^*. \tag{55}$$

---

†*E. G. Ref. 4, p. 148. A matrix* **S** *is called symmetrical when it is identical with the transposed matrix S obtained by interchanging rows of* **S** *with its columns. Proper normalization of the vectors* **a** *and* **b** *means that the factors of proportionality between their components and the electrical quantities are so chosen that* $\frac{1}{2}|a_1|^2$, $\frac{1}{2}|a_2|^2$, $\frac{1}{2}|b_1|^2$ *and* $\frac{1}{2}|b_2|^2$ *represent the mean energy flows in the four waves involved. The values of* r_1 *and* r_2 *are independent of the normalization and so is the product* $t_1 t_2$ *Since (46) and (47) contain* t_1 *and* t_2 *only in the form of their product, so far as slabs are concerned, the normalization is quite immaterial.*

‡*The symbol * indicates the complex conjugate of the quantity it follows.*

§*Cf. Ref. 4, p. 140. A direct proof of (50) can be had by reversing the direction of time and thus interchanging incoming and outgoing waves. This change also replaces every element of* **S** *by its complex conjugate, since time reversal is equivalent to the replacement of j by −j. One obtains in this way* $\mathbf{a} = \mathbf{S}^*\mathbf{b}$ *which together with (48) suffices to establish (50).*

The equality of the real number on the left of (55) with a pure imaginary on the right implies that they are both zero, therefore

$$|r_1| = |r_2| \tag{56}$$

and $t_1 t_2^*$ is real. In fact, from (52) follows: $t_1 t_2^* = 1 - |r_2|^2 \geq 0$ because $|r_2|$ cannot exceed one. Therefore $\arg t_1 = \arg t_2$. Let $\rho = |r_1|$ and $\tau = \sqrt{t_1 t_2^*} = \sqrt{1 - \rho^2}$. One may write:

$$r_1 = \rho\, e^{-j\rho'}, \; r_2 = \rho\, e^{-j\rho''}, \; t_1 = q\tau e^{-j\tau'}, \; t_2 = q^{-1}\tau e^{-j\tau'}, \tag{57}$$

where the positive factor q depends only on the normalization† of the amplitudes. From (53) then follows:

$$\exp j(-\rho' + \tau') = -\exp j(\rho'' - \tau') = \exp j(\rho'' - \tau' + \pi). \tag{58}$$

Hence:

$$\rho' + \rho'' - 2\tau' = \pm\pi. \tag{59}$$

This last relation is of fundamental importance. In the case of a dielectric sheet in air $\rho' = \pi$, $\rho'' = 0$ and $\tau' = 0$. In the case of metal-plate media ρ', ρ'' and τ' depend on the frequency.

It has been assumed so far that the origin is located at the discontinuity. This condition will now be removed and the concept of discontinuity generalized in preparation for the discussion of slabs.

The position of the origin is physically immaterial, a shift of the origin leaves the magnitudes of the reflection and transmission coefficients unchanged. If a new coordinate system is introduced with its origin O′ at (0, 0, l), then $a_1 \exp(-jk_1 z \cos\theta)$ and $a_2 \exp(jk_2 z \cos\theta_2)$ will be replaced by $a_1' \exp(-jk_1 z' \cos\theta)$ and $a_2' \exp(jk_2 z' \cos\theta_2)$ respectively, where, on account of $z = z' + l$

$$a_1' = a_1 e^{-j\phi_1}, \; a_2' = a_2 e^{j\phi_2}$$

with $\phi_1 = k_1 l \cos\theta$, $\phi_2 = k_2 l \cos\theta_2$.‡ Similarly b_1 and b_2 are replaced by $b_1' = b_1 e^{j\phi_1}$ and $b_2' = b_2 e^{-j\phi_2}$ respectively.

The relations between the amplitudes in the two systems of reference can be expressed in a compact form by the use of the matrix

$$\mathbf{P} = \begin{pmatrix} e^{j\phi_1} & 0 \\ 0 & e^{-j\phi_2} \end{pmatrix} \tag{60}$$

---

† *See footnote on p. 17.*

‡ *When this theory is applied to discontinuities in transmission lines $\theta = \theta_2 = 0$ and k_1 and k_2 are the pertinent phase constants of propagation.*

In fact $$\mathbf{a}' = \mathbf{P}^{-1}\mathbf{a},\ \mathbf{b}' = \mathbf{P}\mathbf{b}. \tag{61}$$

Then (48) becomes $$\mathbf{b}' = \mathbf{P}\mathbf{S}\mathbf{P}\mathbf{a}', \tag{62}$$

showing that the shift of origin changed the scattering matrix **S** into **PSP**. Elementary matrix calculation results in:

$$\mathbf{PSP} = \begin{pmatrix} r_1 \exp 2j\phi_1 & t_2 \exp j(\phi_1 - \phi_2) \\ t_1 \exp j(\phi_1 - \phi_2) & r_2 \exp - 2j\phi_2 \end{pmatrix}. \tag{63}$$

In order that the preceding results be valid, it is not necessary that there should be a single plane or point of discontinuity. It is sufficient, that in some part of the space, say, for large negative z, there should be two plane waves progressing in opposite directions (or in directions making angles θ_1 and $\pi - \theta_1$ with the z-axis), and that in another part of the space there should be a similar pair of waves. The amplitudes of these waves should be linearly related and there must be no dissipation of energy so that every process is time reversible. It is clear then that lossless discontinuities located in lossless media can be lumped together into a single lossless discontinuity in the same way as a series of four terminal networks can be lumped together into a single four terminal network. The single discontinuity representing the entire system of discontinuities can then be shifted to any convenient point. The matrices associated with a location of this composite discontinuity are the elements of the matrix family **P S P**, where **S** is the matrix associated with a fixed location of the discontinuity with respect to the coordinate system.

The quantities ϕ_1 and ϕ_2 entering into the definition of **P** have to be determined with some care since it is not at all clear (or relevant) what happens in the neighborhood of the origin where the discontinuities might be located. A shift of the origin must be thought of as a shift of the reference system of the observer, therefore in the equations $\phi_1 = k_1 l \cos\theta$ and $\phi_2 = k_2 l \cos\theta_2$ the appropriate values of k and θ are those which prevail at the site of observation; i.e., far removed from the discontinuity. When, for example, the composite discontinuity consists of a dielectric, or metal-plate slab surrounded by air, then $\phi_1 = \phi_2$, since the observation occurs in air, $k_2 = k_1$, and the emergent beam is parallel to the incident one. This situation prevails for a large class of discontinuities which deserve closer examination.

When a discontinuity possesses a high degree of symmetry this fact is reflected in the matrix **S** provided that the system of reference is properly chosen. In the case of a slab (dielectric, or metal-plate) or a symmetric iris in a waveguide, the plane z = 0 may be made to coincide with the plane of symmetry of the structure. A reversal of the positive direction of z will then leave the matrix **S** unchanged. This reversal is equivalent to an interchange of the indices 1 and 2. Therefore $r_1 = r_2$, $t_1 = t_2$. From (59) then follows:

$$|\rho' - \tau'| = \frac{\pi}{2}. \tag{64}$$

This result is formalized as a theorem.

The phases of the reflection and the transmission coefficients of a symmetric lossless discontinuity differ by 90° provided that the point of reference is the center of symmetry.

In experimental work it is often convenient to refer the phases of the waves involved to one of the physical surfaces of the discontinuity such as the first air-dielectric interface in the case of a dielectric sheet. Let $\mathbf{S}_0$ be the matrix associated with the symmetric discontinuity with the origin located in the plane of symmetry and let d be the over-all thickness of the structure. When the origin is shifted to the front surface, l = -d/2, the matrix

$\mathbf{S}_0$ is replaced by $\mathbf{S} = \mathbf{P}\mathbf{S}_0\mathbf{P}$, with $\phi_1 = \phi_2 = -\frac{1}{2}k\,d\cos\theta$, where k is the propagation constant of the surrounding medium. From (63) follows:

$$\mathbf{S} = \begin{pmatrix} r_1 e^{2j\phi_1} & t_2 \\ t_1 & r_2 e^{-2j\phi_1} \end{pmatrix} \tag{65}$$

therefore $\tau = \tau_0$ and $\rho' = \rho_0' - 2\phi_1 = \rho_0' + dk\cos\theta_0$. It is clear that the quantities ρ, τ and τ' have a physical significance independent of the location of the reference plane. This fact manifests itself mathematically by the invariance of these quantities under the transformation $\mathbf{P}\,\mathbf{S}\,\mathbf{P}$ with $\phi_1 = \phi_2$.

A lossless symmetric discontinuity is electrically characterized by two quantities, say, ρ and τ', since $\tau = \sqrt{1-\rho^2}$ and ρ' has to satisfy (64).† The meaning of two electrical parameters is easily understood. The physical parameters available for adjustment are the series impedance and the shunt reactance. In the familiar case of a dielectric slab there is no energy storage, therefore the shunt reactance in the equivalent circuit is zero. This is, however, not the case for metal-plate slabs.

FORMULAS FOR METAL-PLATE SLABS

A slab of metal-plate medium surrounded by air is a symmetric, approximately lossless discontinuity and the results of the last few paragraphs apply. In order to test the predictions of the Carlson and Heins theory it is sufficient to determine experimentally the magnitude of the reflection coefficient and the phase of either the transmission or the reflection coefficient.

With the aid of equations (57) and (59) one can derive from (46) by elementary manipulations

$$|R| = \frac{2\rho\,|\sin\psi|}{\sqrt{(1-\rho^2)^2 + 4\rho^2\sin^2\psi}}\,, \tag{66}$$

where $\psi = \rho'' + \delta_2$. The absence of loss immediately justifies the equation

$$|T| = \sqrt{1-|R|^2}. \tag{67}$$

From

$$T = |T|e^{-jT'} = \frac{t_1 t_2 \exp j(\delta_1 - \delta_2)}{1 - r_2^2 \exp -j\delta_2}\,, \tag{68}$$

it follows that

$$T' = 2\tau' - \delta_1 + \delta_2 + \arg\left\{1 - \rho^2 \exp\left[-2j(\rho'' + \delta_2)\right]\right\}. \tag{69}$$

---

† *Actually there is an uncertainty in sign resulting in an uncertainty of π in the phase of the reflection coefficient.*

But $$1 - \rho^2 \exp\left[-2j\psi\right] = \left\{(1-\rho^2)\cos\psi + j(1+\rho^2)\sin\psi\right\} \exp\left[-j\psi\right]$$

and therefore

$$\arg\left\{1 - \rho^2 \exp\left[-2j\psi\right]\right\} = \psi' - \psi, \tag{70}$$

where

$$\psi' = \arc\tan\left(\frac{1+\rho^2}{1-\rho^2}\tan\psi\right), \tag{71}$$

and the multiple valued function arc tan x is so chosen that ψ and ψ' lie in the same quadrant. From the last three equations and equation (59) it follows that

$$T' = \rho' + \psi' + \pi - \delta_1. \tag{72}$$

The phase of R, if required, can now be computed with the aid of (64) which applies in this case to the quantities denoted by capital letters.

AMPLITUDE COMPUTATIONS

The numerical computation of $|r|$, $|t|$ and $|r^{(1)}|$ presents no difficulties. First the limiting angle θ_L is found from Figure 4. For $\theta \leqq \theta_L$, $|r|$ is found from (26), $|t|$ from (20) and $r^{(1)} = 0$. For $\theta > \theta_L$, equations (37), (38) and (39) apply. Some care has to be exercised in the neighborhood of the point $\theta = \theta_0$, because all fractions involved are of the form 0/0. This indeterminacy is easily removed by cancelling factors vanishing for $\theta = \theta_0$. With the aid of (41) one may transform (38) to the form:

$$|r| = \frac{1}{4}\frac{(\cos\theta' + \cos\theta)^2}{\cos\theta_0 + \cos\theta}\tan\frac{\theta+\theta_0}{2}\operatorname{cosec}\theta_0 \ . \tag{73}$$

The same procedure is applicable to $|r^{(1)}|$ and $|t|$. Figure 7 shows the values of $\rho = |r|$ plotted against θ for selected fixed values of $x = 2a/\lambda$. Table 1 gives the same information in numerical form and in greater detail. While the shape of the curve $\rho(\theta)$ resembles that of the reflection coefficient of dielectric media for parallel polarization, the curves here plotted do not reach the axis $\rho = 0$.

PHASE COMPUTATIONS

The numerical computation of the phases of the reflection and transmission coefficients is a lengthy, difficult task, even in the simplest case when a diffracted beam is not present. On account of limitations in manpower assigned to this project only those coefficients were computed which have a direct connection with the experimental program undertaken. The results appear at the end of this report.

Since the quantities ρ', ρ'' and τ' satisfy (59), it is sufficient to compute two of these. Only ρ'' enters into the expression for $|R|$, the magnitude of the reflection from a slab of metal-plate material. This is the quantity most easily accessible to measurement and for this reason the major part of the computing effort has been devoted to the computation of ρ'' as a function of $x = 2a/\lambda$ and θ. For normal incidence ρ' was also computed as a function of x. This quantity will be considered first. Next ρ'' will be calculated for normal incidence, finally ρ'' for oblique incidence. In this last case the angle of incidence will be

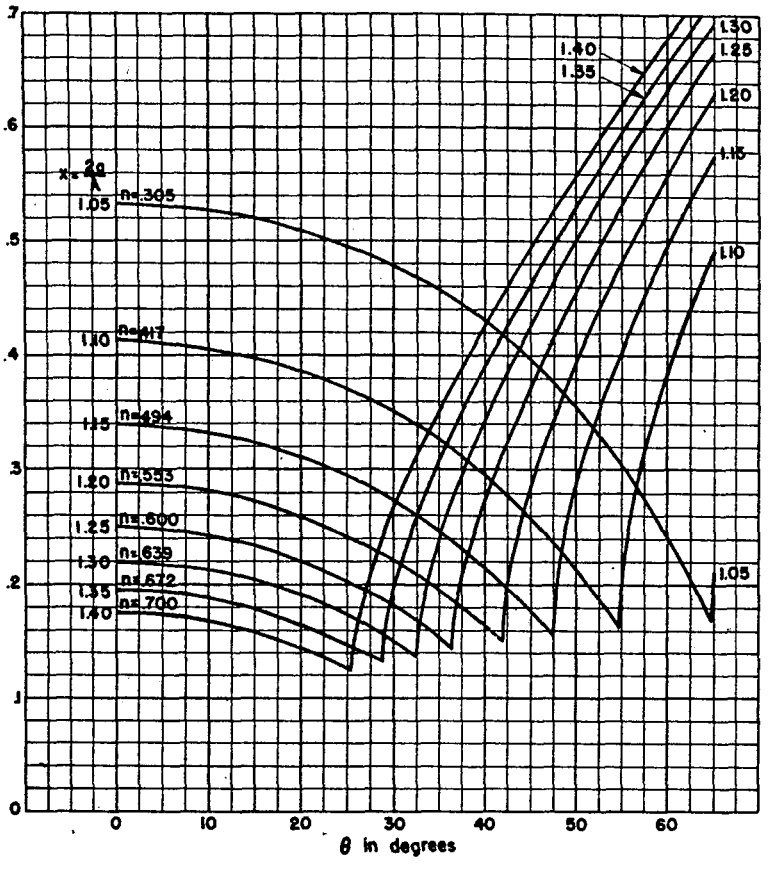

Fig. 7 - Magnitude of the reflection coefficient as a function of angle of incidence (specular reflection)

so restricted that no diffracted beam occurs. The value of ρ' is given by equation (24). In view of equation (9) this can be given the following form:

$$\arg K_+' (-k\cos\theta) = \arg V(-k\cos\theta) + \arg W(-k\cos\theta) - \arg U(-k\cos\theta) - \arg(-k\cos\theta + \kappa)$$
$$- ak\cos\theta\,(\ln 2 - 1)/\pi. \tag{74}$$

When there is only one reflected beam the functions $V(-x)$, $W(-x)$ and $U(-x)$ are complex conjugates of the functions $V(x)$, $W(x)$ and $U(x)$ respectively, moreover $-k\cos\theta + \kappa$ is negative, therefore

$$\arg K_+' (-k\cos\theta) = -\arg K_+ (k\cos\theta) + \pi. \tag{75}$$

When there are two reflected beams (75) is again valid, but one has to verify it separately for $\theta > \theta_0$ and for $\theta < \theta_0$. Consequently,

$$\rho' = 2 \arg K_+ (k\cos\theta). \tag{76}$$

It is now necessary to calculate $\arg K_+(k\cos\theta)$ for the case $\theta = 0$. In this case from (13) and (14) follows:

$$\Delta_n = \Delta_{-n} = \sqrt{1 - \left(\frac{ak}{2\pi n}\right)^2} = \epsilon_{2n}\ , \tag{77}$$

therefore $V(w) = W(w)$. Also $|\Delta_n \pm i(ak/2\pi n)|^2 = 1$.

It is practical to introduce the variable x defined as follows:

$$x = \frac{ka}{\pi} = \frac{2a}{\lambda} \quad . \tag{78}$$

The values of x are limited to the interval 1 to 2. For practical reasons the computations are confined to the range 1.01 to 1.35. From (9) then follows:

$$\arg K_+(k) = 2 \arg V(k) - \arg U(k) + \frac{ak}{\pi}(\ln 2 - 1), \tag{79}$$

where

$$\arg V(k) = -\sum_{n=1}^{\infty} \left(\arc\sin \frac{x}{2n} - \frac{x}{2n}\right), \tag{80}$$

$$\arg U(k) = -\sum_{n=2}^{\infty} \left(\arc\sin \frac{x}{n} - \frac{x}{n}\right). \tag{81}$$

Therefore

$$\arg K_+(k) = x(\ln 2 - 1) - \sum_{n=2}^{\infty} (-)^n \left(\arc\sin \frac{x}{n} - \frac{x}{n}\right) \quad . \tag{82}$$

The last sum can be written in the form $\arc\sin(x/2) - \arc\sin(x/3) - x/6 + R(x)$, where

$$R(x) = \sum_{n=4}^{\infty} (-)^n \left(\arc\sin \frac{x}{n} - \frac{x}{n}\right). \tag{83}$$

The reason for this separation is that R(x) is small. In fact, while x varies from 1.01 to 1.35, R(x) varies from .002 to .004 and the entire expression (82) varies from .33 to .47.

R(x) is calculated by expanding $\arc\sin(x/n)$ in an infinite series and then interchanging the order of summations. This is permissible since all series involved are absolutely convergent. From

$$\arc\sin \frac{x}{n} = \frac{x}{n} + \frac{1}{6}\left(\frac{x}{n}\right)^3 + \frac{3}{40}\left(\frac{x}{n}\right)^5 + \frac{5}{112}\left(\frac{x}{n}\right)^7 + \ldots \tag{84}$$

it follows that

$$R(x) = \frac{1}{6} x^3 \sum_{n=4}^{\infty} \frac{(-)^n}{n^3} + \frac{3}{40} x^5 \sum_{n=4}^{\infty} \frac{(-)^n}{n^5} + \ldots \quad . \tag{85}$$

The summations can now be carried out since the function $\eta(s) = \sum_{n=4}^{\infty} (-)^n n^{-s}$ is related to the Zeta function of Riemann and its values for s = 3, 5, 7, etc. can be found with the aid of the tables of the latter.

Table of the Auxiliary Function
$\eta(s)$

s	3	5	7	9	11
η	.010 4943	.000 7454	.000 0504	.000 0034	.000 0002

The numerical form of R(x) is:

$$R(x) = (17490x^3 + 559x^5 + 22x^7 + x^9 + \ldots) \cdot 10^{-7}, \tag{86}$$

while

$$\arg K_+(k) = -.140\ 1861\ x - \arcsin\frac{x}{2} + \arcsin\frac{x}{3} - R(x). \tag{87}$$

In order to achieve the necessary symmetry for the calculation of ρ'' for normal incidence, the origin has to be moved to a point half-way between the edges, such as the point Q in Figure 2. When this is done the expression for the phase of transmission coefficient becomes in place of (21):

$$\tau' = \arg K_+(k\cos\theta) - \arg K_+(\kappa). \tag{88}$$

Therefore, in view of (59) and (76)

$$\rho'' = 2\tau' - \rho' + \pi = -2K_+(\kappa) + \pi. \tag{89}$$

It is therefore necessary to calculate $K_+(\kappa)$. For normal incidence the procedure is similar to the calculation of $K_+(\kappa)$. However, in the present case the convenient auxiliary variable is $y = nx = \kappa a/\pi$.

From:

$$\left|\Delta_n \pm i\frac{a\kappa}{2\pi n}\right|^2 = 1 - \left(\frac{ak}{2\pi n}\right)^2 + \left(\frac{a\kappa}{2\pi n}\right)^2 = 1 - \left(\frac{1}{2n}\right)^2$$

it follows that

$$\arg V(\kappa) = -\sum_{n=1}^{\infty}\left(\arcsin\frac{y/2n}{\sqrt{1-(2n)^{-2}}} - \frac{y}{2n}\right). \tag{90}$$

Moreover $\arg W(\kappa) = \arg V(\kappa)$, since in the case of normal incidence $V(w) = W(w)$.

Similarly:

$$\arg U(\kappa) = -\sum_{n=2}^{\infty}\left(\arcsin\frac{y/n}{\sqrt{1-n^{-2}}} - \frac{y}{n}\right). \tag{91}$$

Hence

$$\arg K_+(\kappa) = y(\ln 2 - 1) - \sum_{n=2}^{\infty}(-)^n\left(\arcsin\frac{y}{\sqrt{n^2-1}} - \frac{y}{n}\right). \tag{92}$$

The sum is again split as follows:

$$\text{arc sin } y/\sqrt{3} - \text{arc sin } y/\sqrt{8} - y/6 + S(y),$$

where

$$S(y) = \sum_{n=4}^{\infty} (-)^n \left(\text{arc sin } \frac{y}{\sqrt{n^2 - 1}} - \frac{y}{n}\right) . \tag{93}$$

Let

$$u = \frac{y}{\sqrt{n^2 - 1}} = \frac{y}{n}\left(1 - \frac{1}{n^2}\right)^{-1/2}. \tag{94}$$

The binomial theorem gives:

$$u = \frac{y}{n}\left\{1 + \frac{1}{2} n^{-2} + \frac{3}{8} n^{-4} + \ldots\right\},$$

$$u^3 = \frac{y^3}{n^3}\left\{1 + \frac{3}{2} n^{-2} + \frac{15}{8} n^{-4} + \ldots\right\}, \tag{95}$$

$$u^5 = \frac{y^5}{n^5}\left\{1 + \frac{5}{2} n^{-2} + \frac{35}{8} n^{-4} + \ldots\right\}.$$

These expansions may now be substituted in the series of arc sin u. Absolute convergence of all series permits a rearrangement of the terms resulting in the following expression:

$$S(y) = \sum_{n=4}^{\infty} (-)^n y \left\{\frac{1}{2} n^{-3} + \frac{3}{8} n^{-5} + \ldots\right\} +$$

$$+ \frac{1}{6} \sum_{n=4}^{\infty} (-)^n y^3 \left\{n^{-3} + \frac{3}{2} n^{-5} + \ldots\right\} + \tag{96}$$

$$\frac{3}{40} \sum_{n=4}^{\infty} (-)^n y^5 \left\{n^{-5} + \frac{5}{2} n^{-7} + \ldots\right\} + \ldots$$

In a compact form

$$S(y) = g_1 y + \frac{1}{6} g_3 y^3 + \frac{3}{40} g_5 y^5 + \ldots, \tag{97}$$

where

$$g_1 = \frac{1}{2}\eta(3) + \frac{3}{8}\eta(5) + \frac{5}{16}\eta(7) + \ldots = .005\ 5434,$$

$$g_3 = \eta(3) + \frac{3}{2}\eta(5) + \frac{15}{8}\eta(7) + \ldots = .011\ 7153.$$

Similar expressions give for g_5, g_7 and g_9, 8878, 679 and 46 ten-millionths respectively.

The numerical form of the remainder is:

$$S(y) = (55434y + 19525y^3 + 666y^5 + 30y^7 + 2y^9 + \ldots) \cdot 10^{-7}. \tag{98}$$

The final expression for $K_+(\kappa)$ is

$$\arg K_+(\kappa) = -\arcsin y/\sqrt{3} + \arcsin y/\sqrt{8} - .140\,1861 - S(y). \tag{99}$$

In order to obtain ρ'' for $\theta \neq 0$, values of $K_+(\kappa)$ for oblique incidence are required. These were obtained by calculating the difference between $K_+(\kappa,\theta)$ and $K_+(\kappa, 0)$ where the latter is the function designated heretofore by $K_+(\kappa)$.

Since U(w) does not depend on θ

$$\arg K_+(\kappa,\theta) - \arg K_+(\kappa, 0) = \arg V(\kappa, \theta) + \arg W(\kappa, \theta) - 2 \arg V(\kappa, 0). \tag{100}$$

From (13) it follows that

$$\left|\Delta_n + \frac{ia\kappa}{2\pi n}\right|^2 = \left(1 - \frac{ak \sin\theta}{2\pi n}\right)^2 - \frac{1}{4n^2}. \tag{101}$$

Let $v = (ak/\pi)\sin\theta = x \sin\theta$, then

$$\arg V(\kappa,\theta) = -\sum_{n=1}^{\infty}\left(\arcsin \frac{y}{\sqrt{(2n - v)^2 - 1}} - \frac{y}{2n}\right). \tag{102}$$

and

$$\arg W(\kappa, \theta) = -\sum_{n=1}^{\infty}\left(\arcsin \frac{y}{\sqrt{(2n + v)^2 - 1}} - \frac{y}{2n}\right). \tag{103}$$

Introduce the function $f_n(v) = \arcsin y \left[(2n + v)^2 - 1\right]^{-\frac{1}{2}}$. The right side of (100) then becomes

$$-\sum_{n=1}^{\infty} f_n(v) + f_n(-v) - 2 f_n(0).$$

The summand is the second difference of the function $f_n(v)$. It is equal to $f_n''(0)v^2$ plus terms of higher order in v^2. But $f_n''(0)$ is approximately $y/4n^3$, when 1 and y^2 can be neglected in comparison to $4n^2$. In the range of interest $y<1$. Therefore, when N is such that $1 \ll 4N^2$, the following approximation holds

$$\sum_{n=N}^{\infty} f_n(v) + f_n(-v) - 2 f_n(0) = \frac{yv^2}{4}\sum_{n=N}^{\infty} n^{-3}. \tag{104}$$

The terms corresponding to n = 1, 2, 3 and 4 were computed on the automatic computing machine of the Operational Research Branch for angles of incidence θ ranging from 0 to 35° in 5° intervals. The remainder term

$$\frac{yv^2}{4}\sum_{n=5}^{\infty} n^{-3} = .006099yv^2 \tag{105}$$

was then added. The values of $\rho'' - \pi = -2\,K_+(\kappa,\theta)$ are tabulated to four places, except for $\theta = 35°$ in which case only three place accuracy is available.

THE TABLES AND THEIR USE

Table 1 contains $\rho = |r|$ as a function of $x = 2a/\lambda$ from 1.01 to 1.35 and the angle of incidence θ from 0° to 60°. In Table 2 the values of $\rho'' - \pi$ are tabulated for $x = 1.01$

to 1.35 and for $\theta = 0^0$ to 35^0, the approximations adopted not being satisfactory for large values of θ.

A more extensive table was prepared for the case of normal incidence with values of x ranging from 1.01 to 1.35. This presentation (Table 3) also contains the functions $\rho'/2\pi$ and $\rho''/2\pi$ which are useful in practical computations.

As an example for the use of these functions one might consider the computation of the phase change in transmission through a sheet.

Equation (72) can be put in the following form:

$$\frac{T'}{2\pi} = \frac{\rho'}{2\pi} + \frac{1}{2} - \frac{d \cos\theta}{\lambda} + \frac{\psi}{2\pi} + \frac{\psi' - \psi}{2\pi} \quad . \tag{106}$$

Here

$$\frac{\psi}{2\pi} = \frac{\rho''}{2\pi} + \frac{nd}{\lambda}, \tag{107}$$

since the rays are constrained in the metal-plate medium so that $\theta_2 = 90^0$. Having the angle in the form $\psi/2\pi$ is convenient, for ψ is often quite large.

The difference $\psi' - \psi$ is generally small. It can be computed quickly as follows: Let $F = (1 + \rho^2)/(1 - \rho^2)$, then according to (71) $\tan\psi' = F \tan\psi$, therefore

$$\psi' - \psi \approx \tan(\psi' - \psi) = \frac{\tan\psi' - \tan\psi}{1 + \tan\psi' \tan\psi} = \frac{F - 1}{\cot\text{an}\,\psi + F \tan\psi}, \tag{108}$$

provided F - 1 is small.

No detailed tables were prepared for the power division at the air-metal-plate interface. Figure 5 contains the available information.

Table 4 gives the direction of the first diffracted beam as a function of x and the angle of incidence. It also contains the angle $\theta_0 = \arccos n$ as a function of x. This is the angle of incidence for which the interesting equidistribution of power noticed by L. J. Chu takes place.

ACKNOWLEDGMENTS

Professor L. J. Chu of M.I.T., acting as consultant to the Naval Research Laboratory, contributed to the work on this problem by many informal discussions. Mr. C. H. Crisman of the Operational Research Branch, Radio Division III of NRL has generously given time and effort to large scale automatic machine computation of auxiliary functions. The author is indebted to these scientists for their contributions as well as to many of his colleagues in the Antenna Research Branch who supported the work leading to this publication.

TABLE 1
Magnitude of the Reflection Coefficient ρ for Varying Angle of Incidence

$x = \frac{2a}{\lambda}$	$\theta = 0$	5°	10°	15°	20°	25°	30°
1.01	.7538	.7530	.7505	.7462	.7401	.7318	.7210
1.02	.6708	.6697	.6665	.6611	.6533	.6428	.6293
1.03	.6134	.6122	.6086	.6025	.5937	.5818	.5666
1.04	.5690	.5677	.5638	.5572	.5476	.5348	.5184
1.05	.5327	.5313	.5272	.5201	.5100	.4965	.4792
1.06	.5019	.5005	.4961	.4888	.4782	.4642	.4462
1.07	.4752	.4737	.4692	.4617	.4508	.4362	.4176
1.08	.4517	.4502	.4456	.4378	.4266	.4117	.3926
1.09	.4307	.4292	.4245	.4165	.4050	.3898	.3704
1.10	.4118	.4102	.4055	.3973	.3857	.3702	.3504
1.11	.3947	.3931	.3882	.3799	.3681	.3524	.3323
1.12	.3790	.3774	.3724	.3640	.3520	.3361	.3158
1.13	.3646	.3629	.3579	.3494	.3373	.3212	.3006
1.14	.3512	.3495	.3445	.3359	.3237	.3074	.2867
1.15	.3388	.3371	.3321	.3234	.3110	.2946	.2737
1.16	.3273	.3256	.3205	.3118	.2993	.2827	.2617
1.17	.3166	.3148	.3096	.3009	.2883	.2716	.2504
1.18	.3065	.3047	.2995	.2907	.2780	.2612	.2399
1.19	.2970	.2952	.2900	.2811	.2684	.2515	.2301
1.20	.2880	.2863	.2810	.2721	.2592	.2423	.2208
1.21	.2796	.2778	.2725	.2635	.2507	.2336	.2120
1.22	.2716	.2698	.2645	.2555	.2426	.2255	.2038
1.23	.2640	.2622	.2569	.2478	.2349	.2177	.1959
1.24	.2568	.2550	.2497	.2406	.2276	.2103	.1885
1.25	.2500	.2482	.2428	.2337	.2206	.2034	.1815
1.26	.2435	.2417	.2363	.2271	.2140	.1967	.1748
1.27	.2373	.2355	.2300	.2209	.2077	.1904	.1684
1.28	.2314	.2295	.2241	.2149	.2017	.1843	.1623
1.29	.2257	.2239	.2184	.2092	.1960	.1785	.1564
1.30	.2203	.2185	.2130	.2037	.1905	.1730	.1509
1.31	.2151	.2133	.2078	.1985	.1852	.1677	.1455
1.32	.2101	.2083	.2028	.1935	.1802	.1626	.1404
1.33	.2053	.2035	.1980	.1887	.1754	.1578	.1355
1.34	.2007	.1989	.1934	.1841	.1707	.1531	*.1737
1.35	.1963	.1945	.1890	.1796	.1662	.1486	*.1980

*Second lobe present.

TABLE 1
-continued-

x	35°	40°	45°	50°	55°	60°
1.01	.7074	.6903	.6687	.6415	.6068	.5616
1.02	.6122	.5908	.5641	.5307	.4886	.4346
1.03	.5474	.5235	.4938	.4569	.4107	.3521
1.04	.4978	.4722	.4405	.4012	.3524	.2909
1.05	.4575	.4306	.3974	.3565	.3058	.2423
1.06	.4236	.3957	.3614	.3193	.2672	.2024
1.07	.3944	.3658	.3306	.2875	.2344	.1686
1.08	.3688	.3395	.3037	.2598	.2059	*.2801
1.09	.3461	.3163	.2798	.2353	.1808	*.3370
1.10	.3258	.2955	.2585	.2135	*.1849	*.3771
1.11	.3073	.2767	.2393	.1939	*.2709	*.4086
1.12	.2905	.2596	.2218	.1761	*.3150	*.4345
1.13	.2751	.2439	.2059	.1598	*.3479	*.4566
1.14	.2609	.2294	.1912	*.2347	*.3747	*.4758
1.15	.2478	.2161	.1776	*.2776	*.3973	*.4927
1.16	.2356	.2037	.1650	*.3085	*.4169	*.5078
1.17	.2242	.1921	.1533	*.3335	*.4342	*.5214
1.18	.2135	.1813	*.2227	*.3547	*.4497	*.5338
1.19	.2036	.1712	*.2582	*.3732	*.4638	*.5452
1.20	.1942	.1617	*.2845	*.3896	*.4766	*.5557
1.21	.1853	.1528	*.3062	*.4044	*.4883	*.5654
1.22	.1770	*.1793	*.3248	*.4179	*.4992	*.5744
1.23	.1690	*.2215	*.3412	*.4302	*.5093	*.5829
1.24	.1615	*.2481	*.3559	*.4416	*.5187	*.5908
1.25	.1544	*.2691	*.3693	*.4522	*.5275	*.5982
1.26	.1476	*.2870	*.3815	*.4621	*.5358	*.6053
1.27	.1412	*.3026	*.3928	*.4713	*.5436	*.6120
1.28	*.1948	*.3165	*.4033	*.4800	*.5510	*.6183
1.29	*.2206	*.3292	*.4131	*.4882	*.5581	*.6244
1.30	*.2402	*.3408	*.4223	*.4960	*.5647	*.6300
1.31	*.2566	*.3515	*.4310	*.5033	*.5711	*.6356
1.32	*.2709	*.3615	*.4392	*.5104	*.5772	*.6408
1.33	*.2837	*.3709	*.4469	*.5171	*.5830	*.6458
1.34	*.2953	*.3797	*.4543	*.5234	*.5886	*.6506
1.35	*.3060	*.3880	*.4614	*.5296	*.5939	*.6553

*Second lobe present

TABLE 2
Phase of the Back Surface Reflection Coefficient

Table of $\rho'' - \pi$ (in radians)

x	$\theta = 0^\circ$	5°	10°	15°	20°	25°	30°	35°
1.01	.1049	.1064	.1107	.1180	.1284	.1425	.1609	.184
1.02	.1490	.1511	.1573	.1679	.1832	.2038	.2307	.265
1.03	.1832	.1858	.1937	.2070	.2265	.2527	.2869	.331
1.04	.2124	.2155	.2248	.2408	.2639	.2952	.3363	.389
1.05	.2384	.2419	.2527	.2710	.2977	.3340	.3818	.444
1.06	.2622	.2662	.2782	.2990	.3292	.3704	.4248	.496
1.07	.2843	.2888	.3023	.3253	.3590	.4051	.4663	.547
1.08	.3052	.3101	.3249	.3503	.3875	.4586	.5067	.598
1.09	.3250	.3303	.3465	.3742	.4150	.4712	.5465	.648
1.10	.3440	.3498	.3673	.3975	.4418	.5032	.5861	.698
1.11	.3623	.3685	.3874	.4200	.4681	.5348	.6256	.749
1.12	.3799	.3866	.4069	.4420	.4939	.5662	.6652	.802
1.13	.3970	.4042	.4259	.4636	.5194	.5976	.7052	.855
1.14	.4137	.4213	.4445	.4848	.5447	.6290	.7458	.911
1.15	.4300	.4381	.4628	.5058	.5700	.6605	.7872	.968
1.16	.4460	.4546	.4809	.5265	.5951	.6923	.8293	1.028
1.17	.4616	.4708	.4986	.5472	.6202	.7245	.8727	1.091
1.18	.4770	.4866	.5162	.5677	.6454	.7571	.9174	1.158
1.19	.4921	.5022	.5335	.5881	.6707	.7902	.9636	1.229
1.20	.5071	.5177	.5508	.6085	.6964	.8240	1.0115	1.306
1.21	.5218	.5331	.5678	.6289	.7222	.8587	1.0615	1.389
1.22	.5364	.5482	.5849	.6493	.7483	.8941	1.1138	1.480
1.23	.5508	.5632	.6018	.6698	.7747	.9305	1.1688	1.583
1.24	.5650	.5782	.6187	.6904	.8015	.9680	1.2271	1.701
1.25	.5792	.5930	.6356	.7113	.8288	1.0069	1.2893	1.844
1.26	.5932	.6077	.6525	.7323	.8567	1.0471	1.3560	2.032
1.27	.6072	.6223	.6693	.7532	.8850	1.0888	1.4282	2.391
1.28	.6211	.6369	.6862	.7744	.9140	1.1323	1.5074	2.537
1.29	.6349	.6515	.7031	.7960	.9437	1.1781	1.5963	2.523
1.30	.6486	.6660	.7200	.8178	.9743	1.2261	1.6976	2.509

TABLE 3
Tables for Normal Incidence

$x=\frac{2a}{\lambda}$	n	ρ	ρ'	$\frac{\rho'}{2\pi}$	$\rho''-\pi$	$\frac{\rho''}{2\pi}$
1.01	.14037	.7538	-.6589	-.10487	.1049	.51670
1.02	.19706	.6708	-.6663	-.10605	.1490	.52371
1.03	.23959	.6134	-.6738	-.10724	.1832	.52916
1.04	.27467	.5690	-.6813	-.10844	.2124	.53380
1.05	.30491	.5327	-.6889	-.10964	.2384	.53794
1.06	.33167	.5019	-.6955	-.11068	.2622	.54173
1.07	.35575	.4752	-.7041	-.11206	.2843	.54525
1.08	.37770	.4517	-.7117	-.11327	.3052	.54857
1.09	.39789	.4307	-.7194	-.11450	.3250	.55173
1.10	.41660	.4118	-.7271	-.11573	.3440	.55475
1.11	.43403	.3947	-.7349	-.11696	.3623	.55766
1.12	.45034	.3790	-.7427	-.11821	.3799	.56047
1.13	.46567	.3646	-.7506	-.11946	.3970	.56319
1.14	.48014	.3512	-.7585	-.12071	.4137	.56585
1.15	.49382	.3388	-.7664	-.12197	.4300	.56844
1.16	.50679	.3273	-.7744	-.12324	.4460	.57098
1.17	.51912	.3166	-.7824	-.12452	.4616	.57347
1.18	.53086	.3065	-.7905	-.12581	.4770	.57592
1.19	.54207	.2970	-.7986	-.12710	.4921	.57832
1.20	.55277	.2880	-.8067	-.12840	.5071	.58070
1.21	.56302	.2796	-.8150	-.12971	.5218	.58305
1.22	.57283	.2716	-.8232	-.13102	.5364	.58536
1.23	.58225	.2640	-.8316	-.13235	.5508	.58766
1.24	.59130	.2568	-.8399	-.13368	.5650	.58993
1.25	.60000	.2500	-.8484	-.13502	.5792	.59218
1.26	.60837	.2435	-.8569	-.13637	.5932	.59442
1.27	.61644	.2373	-.8654	-.13773	.6072	.59664
1.28	.62422	.2314	-.8740	-.13910	.6211	.59884
1.29	.63172	.2257	-.8827	-.14048	.6349	.60104
1.30	.63897	.2203	-.8914	-.14187	.6486	.60323
1.31	.64597	.2151	-.9002	-.14327	.6623	.60540
1.32	.65275	.2101	-.9091	-.14468	.6759	.60758
1.33	.65930	.2053	-.9180	-.14610	.6895	.60974
1.34	.66564	.2007	-.9270	-.14753	.7031	.61191
1.35	.67179	.1963	-.9360	-.14898	.7167	.61406

TABLE 4
Azimuth of the First Diffracted Beam and the Angle
θ_o = arc cos n.

$x = \frac{2a}{\lambda}$	θ_o	Values of θ' in degrees						
		$\theta = 35^\circ$	$\theta = 40^\circ$	$\theta = 45^\circ$	$\theta = 50^\circ$	$\theta = 55^\circ$	$\theta = 60^\circ$	$\theta = 65^\circ$
1.05	72.25							86.81
1.06	70.63							78.66
1.07	69.16							74.33
1.08	67.81						80.34	71.00
1.09	66.55						75.66	68.21
1.10	65.38					87.48	72.20	65.77
1.11	64.28					79.31	69.35	63.57
1.12	63.23					75.14	66.88	61.57
1.13	62.25					71.95	64.67	59.72
1.14	61.31				81.24	69.27	62.67	58.00
1.15	60.41				76.68	66.92	60.82	56.39
1.16	59.55				73.35	64.82	59.11	54.87
1.17	58.73				70.62	62.91	57.50	53.43
1.18	57.94			81.04	68.26	61.14	55.99	52.03
1.19	57.18			76.80	66.15	59.49	54.55	50.75
1.20	56.44			73.65	64.24	57.94	53.19	49.50
1.21	55.74			71.05	62.48	56.49	51.89	48.30
1.22	55.05		85.24	68.79	60.84	55.10	50.65	47.14
1.23	54.39		79.49	66.77	59.31	53.79	49.46	46.03
1.24	53.75		75.96	64.93	57.87	52.54	48.32	44.96
1.25	53.13		73.18	63.24	56.51	51.34	47.22	43.92
1.26	52.53		70.82	61.67	55.21	50.19	46.16	42.92
1.27	51.94		68.75	60.19	53.98	49.08	45.14	41.95
1.28	51.38	81.47	66.88	58.80	52.79	48.03	44.15	41.01
1.29	50.82	77.64	65.18	57.49	51.66	46.99	43.19	40.10
1.30	50.28	74.77	63.60	56.24	50.57	46.00	42.26	39.21
1.31	49.76	72.39	62.12	55.05	49.52	45.04	41.35	38.35
1.32	49.25	70.32	60.73	53.91	48.51	44.11	40.48	37.51
1.33	48.75	68.46	59.43	52.81	47.54	43.20	39.62	36.62
1.34	48.27	66.77	58.18	51.76	46.59	42.33	38.79	35.89
1.35	47.79	65.22	57.00	50.75	45.68	41.48	37.99	35.11

REFERENCES

1. Cady, W. M., Karelitz, M. B., and Turner, L. A., "Radar Scanners and Radomes," Rad. Lab. Ser. Vol. 26, New York: McGraw-Hill, 1948.

2. Carlson, J. F. and Heins, A. E., "The Reflection of an Electromagnetic Plane Wave by an Infinite Set of Plates I," Quart. Appl. Math. 4, 313-329, 1947.

3. Kock, W. E., "Metal-Lens Antennas," Proc. IRE 34, 828-836, 1946.

4. Montgomery, C. G., Dicke, R. H., and Purcell, E. M., "Principles of Microwave Circuits," Rad. Lab. Ser. Vol. 8, New York: McGraw-Hill, 1948.

5. Stützer, O., Polarizations und Sperrgitter für Zentimeterwellen, Jahrb. d. deutschen Luftfahrtforsch, III, 41-45, 1939.

6. Stützer. O., "Metallinsen für Zentimeterwellen," Z.W.B. No. FB911, German wartime report, 1939.

7. Stützer, O., Artificial Dielectric Optics for Microwaves," AMC Tech. Report No. F-TR-2221-ND (Restricted), December 1948.

* * *

APPENDIX

Calculation of the Magnitude of the Reflection and Transmission Coefficients

In order to find the magnitudes of certain coefficients occurring on pages 8-11, it is necessary to evaluate the absolute value of the complex function $K_+(w)$ and its derivative for certain special values of the variable w. In particular, $|K_+(w)|$ is needed for $w = k\cos\theta$ and κ, while $|K_+'(w)|$ is needed for $w = k\cos\theta$ and $-k\cos\theta'$. Direct substitution in the infinite products defining $K_+(w)$ leads to extremely cumbersome expressions; a somewhat different method is therefore preferable.

The functions $K_+(w)$ and $K_-(w)$ are defined by (9) and (15). On multiplying their absolute values the following equation results:

$$\left|K_+(w)\,K_-(w)\right| = \frac{a}{2}\left|\frac{w + k\cos\theta}{w - k\cos\theta}\,\frac{w-\kappa}{w+\kappa}\right|\left|\frac{V(w)}{V(-w)}\right|\left|\frac{W(w)\,U(-w)}{W(-w)U(w)}\right|. \tag{1A}$$

In view of (8) the left side of (1A) might also be written as $|f(w)\left[K_+(w)\right]^2|$.

When w is real, the last factor on the right of (1A) is always one, since $W(-w) = W(w)^*$ and $U(-w) = U(w)^*$. When Δ_1 is real then also $V(-w) = V(w)^*$ and in this case

$$|f(w)|\;|K_+(w)|^2 = \frac{a}{2}\left|\frac{w + k\cos\theta}{w - k\cos\theta}\,\frac{w-\kappa}{w+\kappa}\right|. \tag{2A}$$

When Δ_1 is imaginary but Δ_2 is real, for every real w

$$\left|\frac{V(w)}{V(-w)}\right| = \left|\frac{k\cos\theta' + w}{k\cos\theta' - w}\right|$$

and therefore

$$|f(w)|\;|K_+(w)|^2 = \frac{a}{2}\left|\frac{w + k\cos\theta}{w - k\cos\theta}\right|\left|\frac{w-\kappa}{w+\kappa}\right|\left|\frac{w + k\cos\theta'}{w - k\cos\theta'}\right|. \tag{3A}$$

To derive an expression for $|K_+(k\cos\theta)|$, it is only necessary to multiply (2A) or (3A) by $(w - k\cos\theta)$ and then let w tend to $k\cos\theta$. According to L'Hospital's rule

$$\lim_{w\to k\cos\theta} f(w)(w - k\cos\theta) = 1/ak\cos\theta,$$

therefore

$$|K_+(k\cos\theta)|^2 = a^2k^2\cos^2\theta\;\frac{k\cos\theta - \kappa}{k\cos\theta + \kappa} \tag{4A}$$

when Δ_1 is real and

$$|K_+(k\cos\theta)|^2 = a^2k^2\cos^2\theta\;\frac{k\cos\theta - \kappa}{k\cos\theta + \kappa}\,\frac{\cos\theta + \cos\theta'}{\cos\theta - \cos\theta'} \tag{5A}$$

when Δ_1 is imaginary.

The omission of the absolute value signs on the right of (4A) and (5A) is justified in view of the fact that $\cos\theta > n$ for real Δ_1 and that for imaginary Δ_1, $n = \cos\theta_0$ lies between $\cos\theta$ and $\cos\theta'$ as seen from (41).

The calculation of $|K_+(\kappa)|$ requires the evaluation of the limit:

$$\lim_{w\to\kappa} \frac{f(w)}{w-\kappa} = \frac{1}{\sqrt{k^2-\kappa^2}} \frac{1}{\cos a\sqrt{k^2-\kappa^2} - \cos(ak\sin\theta)} \lim_{w\to\kappa} \frac{\sin a\sqrt{k^2-w^2}}{w-\kappa} .$$

Since $k^2 - \kappa^2 = \pi^2/a^2$ this limit becomes

$$\frac{a^3\kappa}{\pi^2} \frac{1}{1+\cos(ak\sin\theta)} .$$

Therefore

$$|K_+(\kappa)|^2 = \frac{\pi^2}{4a^2\kappa^2} \frac{k\cos\theta+\kappa}{k\cos\theta-\kappa} \left[1+\cos(ak\sin\theta)\right] \tag{6A}$$

when Δ_1 is real and

$$|K_+(\kappa)|^2 = -\frac{\pi^2}{4a^2\kappa^2} \frac{k\cos\theta+\kappa}{k\cos\theta-\kappa} \frac{k\cos\theta'+\kappa}{k\cos\theta'-\kappa} \left[1+\cos(ak\sin\theta)\right] \tag{7A}$$

when Δ_1 is imaginary.

Since $K_+(w)$ has a simple root at $w = -k\cos\theta$

$$|K'_+(-k\cos\theta)| = \lim_{w\to -k\cos\theta} \frac{K_+(w)}{w+k\cos\theta} . \tag{8A}$$

Equations (2A) and (3A) are divided by $(w + k\cos\theta)$ and the left side is written in the form

$$\left| f(w)(w+k\cos\theta)\left[\frac{K_+(w)}{w+k\cos\theta}\right]^2 \right| .$$

From $\lim_{w\to -k\cos\theta} (w+k\cos\theta)\, f(w) = -1/a\,k\cos\theta$ then follows:

$$|K'_+(-k\cos\theta)|^2 = \frac{a^2}{4} \frac{k\cos\theta+\kappa}{k\cos\theta-\kappa} \tag{9A}$$

when Δ_1 is real and

$$|K'_+(-k\cos\theta)|^2 = \frac{a^2}{4} \frac{k\cos\theta+}{k\cos\theta-\kappa} \frac{\cos\theta-\cos\theta'}{\cos\theta+\cos\theta'} \tag{10A}$$

when Δ_1 is imaginary.

The calculation of $K'_+(-k\cos\theta')$ is similar. In this case

$$\lim_{w\to -k\cos\theta'} f(w)\,(w+k\cos\theta') = -1/a\,k\cos\theta' .$$

Hence

$$|K_+(-k\cos\theta')|^2 = \frac{a^2}{4}\,\frac{k\cos\theta'+\kappa}{k\cos\theta'-\kappa}\,\frac{\cos\theta'-\cos\theta}{\cos\theta'+\cos\theta}\,. \tag{11A}$$

From (23), (4A) and (9A) follows

$$|r| = \frac{k\cos\theta-\kappa}{k\cos\theta+\kappa} \tag{12A}$$

for real Δ_1, while for imaginary Δ_1 (23), (5A) and (10A) give

$$|r| = \frac{k\cos\theta-\kappa}{k\cos\theta+\kappa}\,\frac{\cos\theta+\cos\theta'}{\cos\theta-\cos\theta'}\,. \tag{13A}$$

Expressions for $|t|$ and $r^{(1)}$ are obtained in the same way. The formulas (20), (37) and (39) result.

* * *

NAVY-DPPO-PRNC-WASH.D.C.3739